ACTA RADIOLOGICA
EDITA IUSSU SOCIETATUM RADIOLOGICARUM
DANIAE, FENNIAE, NORVEGIAE ET SUECIAE

VOL. 48 SEPTEMBER 1957 FASC. 3

ROENTGENOLOGIC FEATURES OF FRACTURE OF THE TIBIAL TUBEROSITY

(Osgood-Schlatter's disease)

by

Bengt Hulting

OSGOOD (9) and SCHLATTER (13) independently described the clinical features of the condition named after them. They also demonstrated certain roentgenologic changes, and stressed the traumatic origin of the disease. Many authors have accepted this pathogenetic mechanism (1, 3, 4, 8, 15, 16, 17, 18), whereas others have put forward different theories (5, 6, 7, 10, 12). Descriptions are still found of Osgood—Schlatter's disease as a constitutional anomaly (14) or as an aseptic necrosis of bone with no traumatic background (11).

Few authors have made any detailed study of the roentgenologic features. SUTRO and POMERANZ (16) mentioned soft-tissue swelling at the site of attachment of the ligamentum patellae, 'fragments of bone avulsed from the anterior surface of the tubercle', and 'islands of bone in the patellar ligament at a considerable distance above the tubercle, which may have been formed there or may have been fragments avulsed from the tubercle'. PALUGYAY (10) gave an increased distance between the tuberosity and the tibia, as well as blurring of the margin of the tuberosity, as among the typical changes. HUGHES (4), who regarded Osgood—Schlatter's disease as an intraligamentous condition, stressed

Submitted for publication 4 May 1957.

From the Roentgen Department (Former Director: Docent S. R. Kjellberg), Children's Clinic, Karolinska Sjukhuset, Stockholm, Sweden.

that ossification in the ligamentum patellae or enlargement of the ligamentum patellae at or above the site of insertion, sometimes together with 'abnormal bone' in the ligament, were characteristic roentgenologic features.

The objects of the present investigations were the following:

1. To study the skeletal and soft-tissue changes visible roentgenologically in the tibial tuberosity when it is affected at various stages of development.

2. To contribute to the pathogenesis of the disease by an analysis of the roentgenologic findings.

Normal development of the tibial tuberosity

Complete ossification of the normal cartilage of the tuberosity is known to take place via an apophyseal stage. This is characterized by the appearance in the cartilage of one or several bone centres. Opinions vary greatly as to the time at which this occurs (1, 2, 10, 12, 17).

In order to obtain an idea of the variations in the roentgenologic anatomy of the tuberosity at various developmental stages, this region was studied in practically all patients aged from 7 to 14 years who underwent examination of the knee in our department from 1951 to 1956. They amounted in all to 434 children of both sexes. Cases with symptoms referred to the region of the tuberosity were not included. In almost every case both knees were examined, and skeletal as well as soft-tissue roentgenograms were taken. Since frontal projections give little information about the appearance of the tuberosity, only lateral projections were used for this study. The tuberosity was not examined in any special positions. In most cases only one roentgenologic examination was made.

The cases were classified systematically into the cartilaginous, apophyseal and bony stages. Those cases in which synostosis was established between the apophysis of the tuberosity and the tibial epiphysis were assigned to the bony stage.

The percentage distribution of the respective stages in the different age groups is shown in the following table.

It is seen from this table that the apophyseal and bony stages appeared about two years earlier in girls than in boys. Synostosis between the apophysis of the tuberosity and the tibial epiphysis was established in almost 100 per cent of the girls at 12 years of age, but not until 14 years in the boys.

Cartilaginous stage (Fig. 1 a). The series contained 209 cases with the tuberosity in the cartilaginous stage. The appearance varied little

Table

	Age in years							
Boys	7	8	9	10	11	12	13	14
Cartilaginous stage %	100	100	97	95	75	32	21	—
Apophyseal stage %	—	—	3	5	22	32	21	7
Bony stage %	—	—	—	—	3	36	58	93
Girls								
Cartilaginous stage %	100	85	71	38	7	—	—	—
Apophyseal stage %	—	15	29	28	22	3	—	—
Bony stage %	—	—	—	34	71	97	100	100

in the individual cases. Slight differences were occasionally observed between the two sides in the same individual. Thus, in 9 cases there was a cartilaginous stage on one side and an apophyseal stage on the other. In the late stages of the cartilaginous stage, an ossified projection from the anterior lower part of the tibial epiphysis was generally observed.

Apophyseal stage (Fig. 1 b). This stage was present in 60 cases, including the aforementioned 9. The appearance of the apophysis of the tuberosity varied greatly, owing to the differences in the number of bone centres, their shape and size. At this stage, a small thin bone centre in the lower part of the tuberosity, or occasionally beside the epiphyseal projection, represented initial ossification; in the final stage, a large centre was visible in close contact with the tibial epiphysis.

One bone centre was present in 48 per cent of cases in this group, 2 centres in 23 per cent, 3 or 4 in 15 per cent, and 5 or more in 8 per cent. In 6 per cent of the cases a projection was observed from the tibial metaphysis; it was directed upwards and forwards at the level of the lower part of the tuberosity.

When several bone centres were present, they frequently varied in size, the largest lying most caudally and anteriorly. They were most often arranged in a row, and a line joining their anterior border then formed a continuation of the anterior contour of the epiphysis.

Differences between the number and size of the centres in the two sides of the same individual were present in about two-thirds of the cases. In 5 cases the apophyseal stage was represented on one side and the bony stage on the other and, as already mentioned, the apophyseal stage on one side and the cartilaginous stage on the other in an additional 9 cases. In about one-third of the cases the apophyses had essentially the same appearance on both sides.

In these 'normal cases' the individual centres had an ordinary bone structure and were always well delimited. Thus, no difference was present in the density of the centres that could be ascribed to variations in the bone structure.

Bony stage (Fig. 1 c). This stage was represented in 171 cases, in addition to the aforementioned 5 with the bony stage on one side and the apophyseal stage on the other. In the lateral view, the typical tongue-shaped process representing the tuberosity formed a more or less marked anterior convexity. The surface generally had a completely even contour from the site of synostosis to the tip. Only occasionally did the process show a slightly different outline on comparison of the two sides.

The soft tissues in the region of the tuberosity. The ligamentum patellae, which borders on fat both anteriorly and posteriorly, was distinctly visualized in all three stages of development. The anterior border was generally less distinct than the posterior, owing to the fact that dense streaks were present in the subcutis in many cases. At the level of the tuberosity, the anterior border had a linear outline or possibly a slight forward bulge. In the lateral projection, the fat behind the ligament was seen as a wedge directed downwards; in most cases its tip reached the level of the epiphyseal cartilage.

Pathologic cases

The series comprised 75 cases, 41 boys and 34 girls, referred to our department during the period January 1952 to January 1956 with the diagnosis of Osgood—Schlatter's disease. A few cases with clinical indications of this disease were not included in the series, since tenderness over the tuberosity was lacking, or roentgenologic examination disclosed some other pathologic condition. The right knee was involved in 22 cases, the left in 38 and both knees in 15 cases. A marked difference was present between the boys and girls as to the age of onset, the average age being 12 years in the former and 10 years in the latter.

In 67 of the 75 cases, repeated roentgenologic examinations were made in the course of treatment, and a follow-up examination from 6 months to 4 years after the first examination. In the majority of cases treatment consisted of immobilization in a plaster cast for 4 to 6 weeks. During the last year of the period in question, operation consisting of reduction together with suture of any avulsed fragments was performed in a few cases. An account of the clinical part of the investigation will be published elsewhere by G. EHRENBORG.

Technique

All the knees were depicted in frontal, lateral and oblique views. In addition, soft-tissue roentgenograms were made in the frontal and lateral planes, as well as localized views of the tuberosity in the lateral

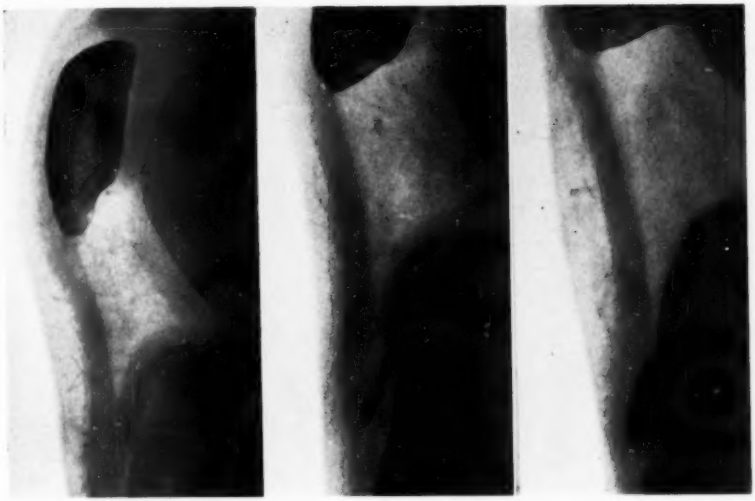

a b c

Fig. 1. The tibial tuberosity at different stages of development, normal cases: a) Cartilaginous, b) apophyseal, and c) bony stage. In all three stages the ligamentum patellae is sharply delimited anteriorly from the subcutaneous fat. Slight forward convexity at the level of the tuberosity. The ligament is also sharply delimited from the fatty tissue behind it, which forms a wedge with its tip pointing downwards. In the apophyseal stage well-defined bone centres with a regular structure and arrangement. In the bony stage the tongue-shaped process given off from the tibia has an even anterior outline with a slight forward convexity.

plane and with slight inward rotation. These latter may be regarded as ideal when the posterior margin of the fibular epiphysis is projected over the posterior margin of the tibia. With insufficient inward rotation of the lower leg, the tuberosity is slightly overlapped, and the wedge of fat behind the ligamentum patellae does not appear so distinctly. Roentgenograms of the unaffected knee were taken for comparison in practically every case. The analyses were based on the observations in the lateral projections.

Roentgenologic observations

It was found suitable from a practical point of view to classify the 75 cases on the basis of the developmental stage of the tibial tuberosity at the first examination.

Group I: Tuberosity in the cartilaginous stage. In all 3 cases in this stage, swelling of the soft tissues was present at the site of the tuberosity in the single examination performed.

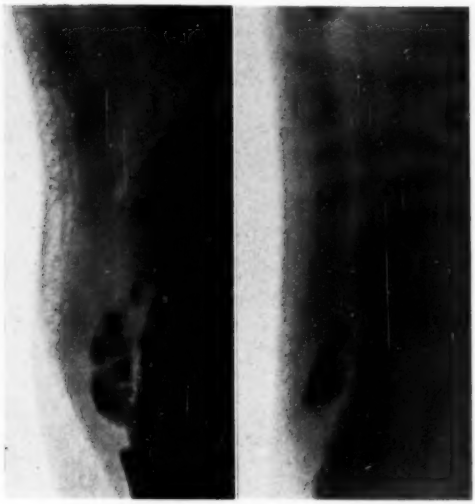

a b

Fig. 2. Boy, aged 11 years. Symptoms present for 6 months, following injury. a) Thickening of soft tissues in front of and above apophysis. Irregular arrangement and structure of bone centres. Anteriorly, a few fragment-like shells. b) Healthy side. No thickening of soft tissues. Centres regularly arranged, with normal bone structure.

Group II: Tuberosity in the apophyseal stage (Figs. 2 and 3). This group comprised 17 cases.

In 14 cases, various changes in the ossified part of the tuberosity were observed in addition to soft-tissue swelling. In some cases irregularities were present in the bone structure, due to an increase in the calcium content of some bone centres or parts of them. In other cases irregularly distributed, sclerotic shells were visible. In 8 cases, there were also fragment-like shells slightly anterior to the bone centres. Finally, in 2 cases a transverse fracture was seen to divide a bone centre into two fragments of equal size, with a distinct diastasis.

At subsequent examinations, osseus deposits on the tuberosity were observed in 4 cases, in addition to ossifications in the overlying soft tissues. In the remaining 10 cases, no pathologic changes were present at follow-up examination. Thus, the tuberosity had an ordinary shape and the bone structure a completely normal appearance.

In the remaining 3 cases in the apophyseal stage the only pathologic feature was soft-tissue swelling over the region of the tuberosity. Repeated examinations were made in 2 of these cases. The swelling gradually subsided, and no other pathologic changes subsequently appeared.

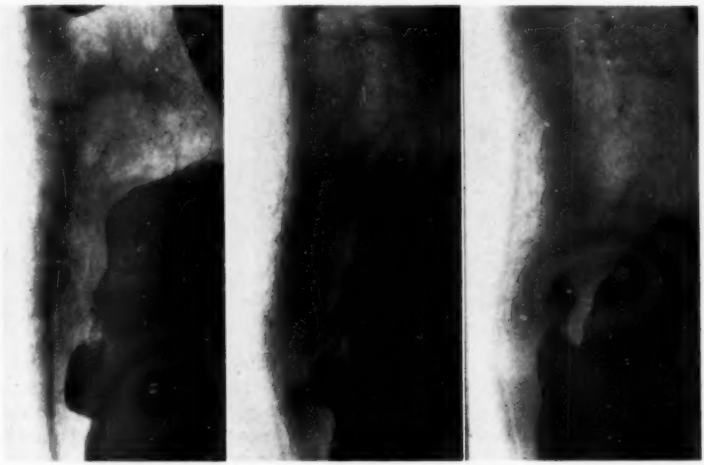

a b c

Fig. 3. Boy, aged 12 years. Duration of symptoms 1 year; no known injury. a) Healthy side. No soft-tissue swelling. Normal bone structure. b) Well-defined soft-tissue swelling. Small fragments separated from superior part of bone centre; displaced slightly forwards. c) 2 years later. Symptoms still present. Deformation of tuberosity. Thickening of lower part of ligamentum patellae. Ossification in soft tissues above the tuberosity.

Group III: Tuberosity in the bony stage (Figs. 4, 5, 6, 7 and 8). This group, which was the largest, comprised 55 cases. In 47 of them, relatively uniform changes were observed in the initial roentgenograms, *i. e.*, swelling of the soft tissues over the tuberosity and one or several fragments in front of it.

In cases with only a few weeks' history, the soft-tissue swelling appeared as an indistinctly delimited density, involving both the subcutaneous tissue over the region of the tuberosity and the wedge of fat behind the ligamentum patellae. This eliminated the normally fairly sharp borderline between the subcutaneous tissue and the ligamentum patellae, as well as a varying proportion of the wedge of fat. In cases with a longer history, the soft-tissue swelling was seen as a thickening of the ligament at the level of the tuberosity, with a more or less marked accentuation of the normally inappreciable forward bulge. In these cases the sharp delimitation from the subcutaneous tissue was present.

The avulsed fragments, which were invariably displaced forwards and upwards, varied in both size and shape. Some consisted of minute, thin shells, whereas others were in the form of more or less rounded bodies, up to 10 mm in diameter. In several cases an irregular defect in

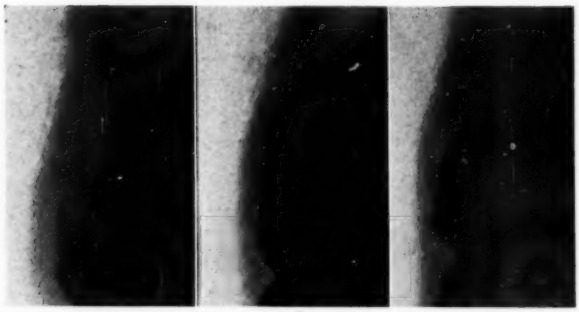

a b c

Fig. 4. Girl, aged 11 years. Sudden onset of pain during high-jump 2 months earlier; symptoms since then. a) Well-defined soft-tissue swelling obliterating the wedge of fat. Shell-like fragment displaced forwards. b) After immobilization in plaster cast for 4 weeks. Slightly decreased soft-tissue swelling. Bone formation in space between fragment and tuberosity. c) 3 weeks later. Asymptomatic after immobilization in plaster cast for altogether 6 weeks. No soft-tissue swelling. Fracture healed. Typical deformation of tuberosity.

the bone was seen in the anterior part of the tuberosity. It was at the level of the avulsed fragment or slightly caudal to it, and of approximately the same shape and size.

Repeated examinations were made in 43 of these 47 cases. During immobilization in plaster, the space between the avulsed fragment and the tuberosity was observed to become successively filled by callus and newly formed bone. In every case the fragment joined in an unchanged position onto the tuberosity, resulting in deformation of its antero-superior aspect.

In 14 of the 43 cases, follow-up examination showed, in addition to deformation of the tuberosity, one or several ossifications in the soft tissues adjacent to it. These patients still had some disability.

In 7 of the 55 cases in this group, soft-tissue swelling, deformation of the tuberosity, as well as one or several usually well-delimited ossifications in the soft tissues, were already present at the first examination. The symptoms had been of long duration in all these patients. Little change in the roentgenograms was seen at the subsequent examinations. In a few cases the ossifications increased in size, and in 2 cases they became united with the tuberosity during immobilization of the knee.

The roentgenologic appearance was normal in one case. The patient was an 11-year-old girl; the symptoms had been present for one month with no definite history of injury, and there was distinct tenderness over the tuberosity. At a follow-up examination one year later, the symptoms

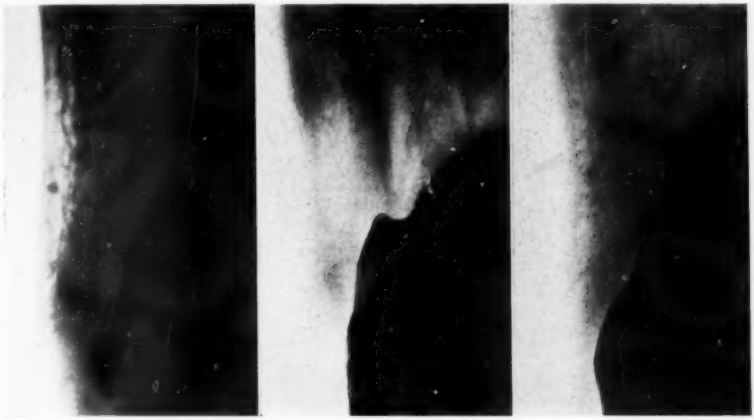

a b c

Fig. 5. Boy, aged 13 years. Symptoms for 1 month; no known injury. a) Diffuse soft-tissue swelling obliterating wedge of fat. Shell-shaped fragment displaced forwards. b) 4 years later. Typical deformation of superior part of tuberosity. c) Healthy side at follow-up examination. Normal appearance.

persisted and distinct tenderness was present on palpation. Roentgenologic examination failed to disclose any pathologic changes in the bone or soft tissues.

Discussion

It has earlier been difficult to establish the pathogenesis of Osgood—Schlatter's disease from roentgenologic observations alone. This is because too little regard has generally been paid to the normal variations in the anatomy of the tibial tuberosity associated with age.

In the present series, an analysis was made of the roentgenologic features in 75 cases with a clinical diagnosis of Osgood—Schlatter's disease. It was then found that the changes were relatively uniform in cases in the same stage of development.

The roentgenologic changes are best explained by the assumption that they represent the sequelae of a fracture of the tuberosity. Thus, in practically every case with the tuberosity in the bony stage, fragments lying outside it were observed. When there has been no direct blow, this displacement can be explained by traction of the ligamentum patellae. At subsequent examinations, the space between the fragment and the tuberosity was seen to become successively filled by callus and newly formed bone, when the knee was immobilized in a plaster cast. After

a b

Fig. 6. Girl, aged 10 years. Acute onset of pain during long-jump 3 weeks earlier; symptoms since then. a) Diffuse soft-tissue swelling obliterating wedge of fat. Minute shell-like fragment of cortex a few millimetres in front of superior part of tuberosity (arrow). b) 3 years later. Symptoms still present. Deformation of superior part of tuberosity. Ossification in soft tissue above it.

healing, characteristic deformation of the antero-superior aspect of the tuberosity persisted, as a result of the original displacement of the fragment. This deformation was more or less conspicuous, but was always fully evident in a comparison with the unaffected knee.

Even in the bony stage, ossification of the tuberosity is not complete at the ages in question here. Consequently, the injury produces not only avulsion of the bone fragments visible in the roentgenogram, but also of the cartilage in front of them. This contributes to the thickening of the tissues over the tuberosity demonstrable both clinically and roentgenologically.

In the cases with the tuberosity in the apophyseal stage, the changes were less conspicuous, and were sometimes difficult to interpret. In about half these cases, fragment-like shells were identified in front of the bone centres, and in a few additional cases there was a transverse fracture of the centre, with diastasis of the fragments. The majority of cases in this group presented, in addition to soft-tissue swelling, an irregular bone structure, with increased density of the bone centres or parts of them. This change in the bone structure is presumably an expression of a circulatory disturbance, and the condition is similar in this respect to a pseudarthrosis.

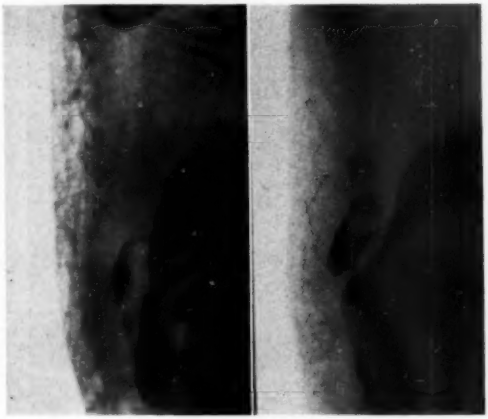

a b

Fig. 7. Girl, aged 10 years. Symptoms present for 2 months, following injury. a) Fairly well-delimited soft-tissue swelling obliterating the wedge of fat. Several fragments displaced forwards and upwards. b) 2 years later. Patient asymptomatic. Typical deformation of tuberosity. Ossification in soft tissues above it.

In some cases with bilateral involvement, only one knee was placed in a plaster cast in order to evaluate the importance of immobilization. Healing took place on the immobilized side, but not on the other.

The history also argues in favour of a traumatic origin. Thus, a definite injury had occurred in 60 per cent of the cases, and in an additional 15 per cent the symptoms had appeared in connexion with games or sports. The most common cause seemed to have been jumping or a direct blow. In many cases the onset was in the form of sudden pain in the 'jumping leg' in a high-jump or long-jump.

This conception of direct or indirect injury as the etiologic factor could be verified at operation. Beside the tuberosity were found separate pieces of cartilage which were firmly adherent to bone fragments; the latter, which exhibited freshly fractured surfaces, were identical in size and shape to those observed at roentgenologic examination.

Ossifications in the soft tissues above the tuberosity were present in about 30 per cent of the cases with the tuberosity in the bony stage, and in a few of those in the apophyseal stage. Various theories have been put forward regarding the mechanism of origin. On the basis of the theory of the pathogenesis presented here, it is probable that in most cases they represent ossification of dislocated fragments of cartilage.

Roentgenologic changes can be demonstrated in practically every case of Osgood—Schlatter's disease. When the tuberosity is in the bony

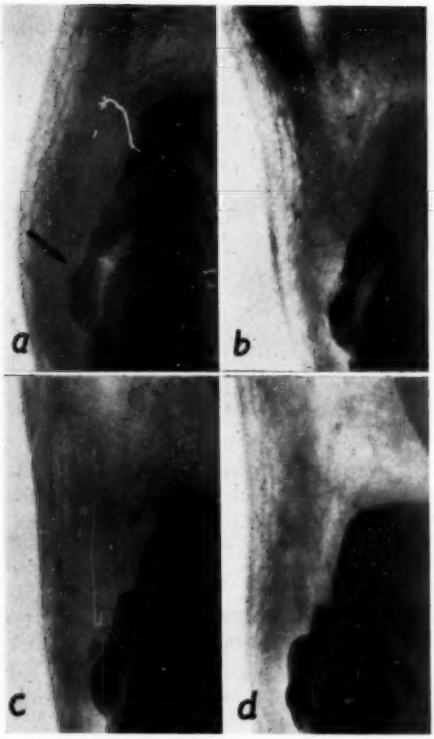

Fig. 8. Boy, aged 12 years. Sudden onset of pain during sprinting 3 months earlier; symptoms since then. a) Fairly well-defined soft-tissue swelling; the wedge of fat cannot be identified. Minute shell-like fragments of cortex slightly displaced forwards (arrow). b) After immobilization in plaster cast for 4 weeks. Inappreciable soft-tissue swelling. Bone formation in space between fragments and tuberosity. c) 4 months later. The symptoms reappeared a few weeks earlier, after fresh trauma. Moderate soft-tissue swelling. Shell-shaped fragments displaced forwards. Small bone defect in anterior part of tuberosity. d) Another 7 months later. Asymptomatic after immobilization in plaster cast for 3 weeks. No soft-tissue swelling. Fracture healed. Typical deformation of tuberosity.

stage, their appearance is almost pathognomonic. The roentgenologic features are also typical in most cases in the apophyseal stage. In the cartilaginous stage, on the contrary, the findings are less evident.

In view of the aforegoing arguments, fracture of the tibial tuberosity seems to be a more apt term for this condition. In our experience, healing takes place with treatment according to current principles of fracture surgery.

SUMMARY

The normal appearances of the tibial tuberosity in the cartilaginous, apophyseal, and bony stages based on the examination of about 400 children aged from 7 to 14 years are described. The roentgen changes in 75 cases with a clinical diagnosis of Osgood—Schlatter's disease were found to be relatively uniform when the tuberosity was in the same stage of development. The changes are best explained by the assumption that they represent the sequelae of a fracture of the tuberosity.

ZUSAMMENFASSUNG

Das normale Aussehen der Tuberositas tibiae im knorpeligen, apophysären und knöchernen Stadium wird auf der Basis einer Untersuchung von etwa 400 Kindern im Alter von 7 bis 14 Jahren beschrieben. Die röntgenologischen Befunde in 75 Fällen mit der klinischen Diagnose Osgood-Schlattersche Krankheit waren verhältnismässig gleichartig, wenn sich die Tuberositas tibiae im gleichen Entwicklungsstadium befand. Die Veränderungen werden am besten durch die Annahme, dass sie die Folgeerscheinung einer Fraktur der Tuberositas sind, erklärt.

RÉSUMÉ

Ayant examiné environ 400 enfants agés de 7 à 14 ans, l'auteur décrit les aspects normaux de la tubérosité tibiale antérieure aux stades cartilagineux, apophysaires et osseux. Dans 75 cas où on avait porté le diagnostic clinique de maladie d'Osgood—Schlatter, les modifications radiologiques ont paru assez uniformes sur des tubérosités au même stade de développement. La meilleure façon d'expliquer ces modifications est de supposer qu'elles représentent les séquelles d'une fracture de la tubérosité.

REFERENCES

1. Dunlop, J.: The adolescent tibial tubercle. Am. J. Orthoped. Surg. 9 (1912), 313.
2. Goff, C. W.: Legg—Calvé—Perthes syndrome and related osteochondrosis of youth. Charles C. Thomas. Springfield 1954.
3. Haglund, P.: Zur Frage der Schlatterschen Krankheit. Ztschr. f. Orthop. 27 (1910), 475.
4. Hughes, E. S. R.: Osgood—Schlatter's disease. Surg. Gynec. Obst. 86 (1948), 323.
5. Jacobsthal, H.: Über die in der Adolescenz auftretende Verdickung der Tuberositas tibiae. Deutsche Ztschr. Chir. 86 (1907), 493.
6. Kienböck, R.: Über Osteochondritis an der Tuberositas tibiae und die sogenannte Osgood—Schlattersche Erkrankung. Fortschr. Röntgenstr. 15 (1910), 135.
7. Kirchner, A.: Zur Frage der juvenilen Fracturen der Tuberositas tibiae, Tuberositas navicularis und des Tuber calcanei. Arch. klin. Chir. 84 (1907), 898.
8. Nagura, S.: Die Pathologie und das Wesen der Schlatterschen Krankheit. Arch. klin. Chir. 198 (1940), 650.
9. Osgood, R. B.: Lesions of the tibial tubercle occurring during adolescence. Boston Med. Surg. J. 148 (1903), 114.

10. Palugyay, J.: Zur Ätiologie und Röntgendiagnose der unter 'Schlatter—Osgood Erkrankung' zusammengefassten Veränderungen der Tuberositas tibiae. Fortschr. Röntgenstr. 35 (1926), 595.
11. Pease, C. N.: Avascular necrosis of bone in children. M. Clin. North America. 34 (1950), 165.
12. Perrot, A.: De l'ossification normale et des manifestations pathologiques de la tuberosité antérieure du tibia. Rev. d'orthop. 20 (1933), 497.
13. Schlatter, C.: Verletzungen des schnabelförmigen Fortsatzes der oberen Tibiaepiphyse. Beitr. klin. Chir. 38 (1903), 874.
14. Seyss, R. und Wiesner, E.: Das Epiphysenwachstum bei der Osgood—Schlatterschen Störung. Ztschr. Orthop. 80 (1950), 623.
15. Smillie, I. S.: Injuries of the knee joint. Livingstone, Edinburgh 1946.
16. Sutro, C. J. and Pomeranz, M. M.: Osgood—Schlatter's disease. Arch. Surg. 31 (1935), 807.
17. Uhry, E.: Osgood—Schlatter's disease. Arch. Surg. 48 (1944), 406.
18. Watson-Jones, R.: Fractures and joint injuries. Livingstone, Edinburgh 1946.

FROM ROENTGEN DEPARTMENT III (DIRECTOR: DOCENT I. WICKBOM), SAHLGRENSKA SJUKHUSET, GOTHENBURG, SWEDEN

HYPERNEPHROMA IN A PELVIC KIDNEY DEMONSTRATED BY ANGIOGRAPHY

Report of a case

by

Osborne Bartley

The frequency of renal ectopia, or congenital malposition of the kidney, as determined from autopsy material is variously stated as lying between 1 in 500 and 1 in 1,100 (4, 14, 13, 3, 1). In a material of 3,285 urologic investigations, THOMAS and BARTON found 6 cases of renal ectopia, which corresponds to a ratio of 1 : 547. The displacement is usual downwards and the condition is distinguished from nephroptosis by a short ureter, an anomalous blood supply, and as a rule by a renal hilum directed forwards. The particular type of renal ectopia represented by the pelvic kidney occurs according to STEVENS in 1 in 2,150 to 3,000 post-mortem examinations.

The present author in a survey of intravenous urographies performed in 10,500 patients from 1953 to 1956 inclusive, in Roentgen Departments I and III of Sahlgrenska Sjukhuset found 9 cases of renal ectopia which thus occurred in 1 in 1,165 urographic examinations. Among these there were 5 cases of pelvic kidney, so that in the whole material the frequency of pelvic kidney was 1 in 2,100 urographies.

According to BELL, processes of disease affect the ectopic kidney to the same extent as the normally placed kidney although hydronephrosis and pyelonephritis are both more common in ectopia. The incidence of hypernephroma in normally situated kidneys is, according to the same author, about 1 % in men and 0.75 % in women. In another autopsy material (2) hypernephroma occurred in about 2 % of the cases. It is

Submitted for publication 1 July 1957.

Fig. 1. Intravenous urography. Left kidney situated in true pelvis in front of sacrum. No deformation of renal pelvis to indicate tumour.

Fig. 2.

Fig. 2. Angiography, arterial phase. Rounded tumour about the size of a mandarin, rich in vessels (←). The kidney is supplied by two wide arteries from the region of the bifurcation of the aorta (↞). Branches from the inferior mesenteric artery (↞) partly project over the kidney but apparently do not contribute to its vascular supply. (Cf. Fig. 3 top.)

evident that these figures are not entirely representative since they are based upon selected materials but they nevertheless afford an approximate indication of the incidence of hypernephroma in renal ectopia.

It may be inferred from what has been said above that a malignant growth seldom occurs in a case of ectopic kidney, and in fact the cases described in the literature are few and far between. Only 10 cases seem to have been published, as far as I have been able to ascertain, and consist of 6 cases of crossed ectopia reported by McKenzie & Hawthorne, Patch, Langworthy & Drexler (2 cases), Lee, and Ultzmann, and 4 cases of pelvic kidney reported by Wulff, Young, Campbell, and Earlam et coll. The cases published by the three first-mentioned authors had been observed at autopsy while the case of Earlam et coll. was demonstrated at operation. In some of these 10 cases urography or retro-

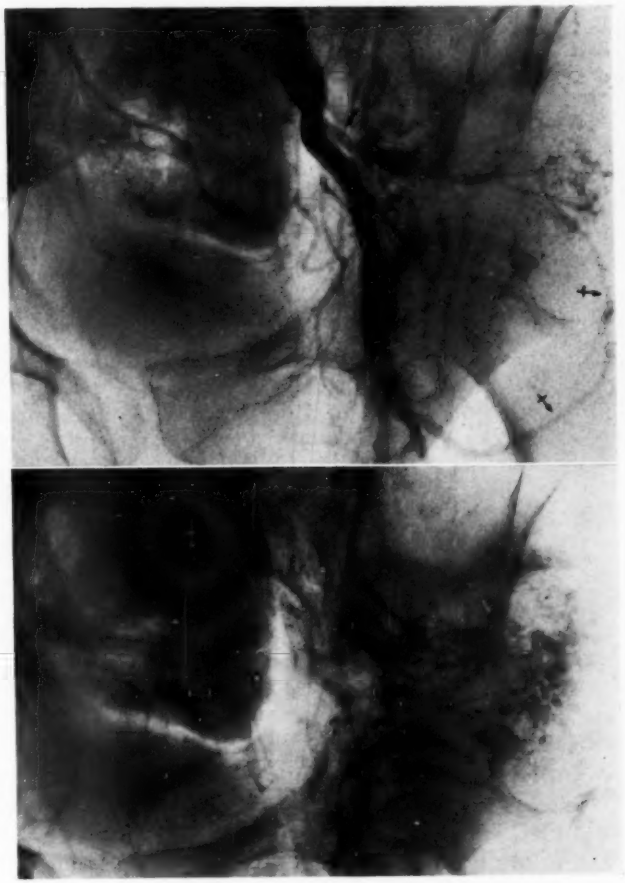

Fig. 3. *Top:* Arterial phase. *Bottom:* About 3 sec later. Numerous tumour vessels with arteriovenous fistulae lie in the area of the bone destruction and surrounding soft parts. The vascular supply of the metastasis is derived partly from the wide superior gluteal artery (←) and partly from the dilated superficial circumflex iliac artery (↔).

a

b

Fig. 4. Specimen. a) Arrows indicate the hypernephroma in the ectopic kidney. b) The kidney cut open.

grade pyelography had been performed without a definite diagnosis being established. Renal angiography does not appear to have been employed in any instance and there therefore seems to be some justification for reporting a case in which the diagnosis of a hypernephroma in a pelvic kidney was made by means of renal angiography, and in which tumour vessels in a metastasis in the bony pelvis were demonstrated at the same time. This is probably the fifth of the known cases of a malignant tumour in a pelvic kidney and the first one to have been diagnosed roentgenologically.

Case report

A male, aged 52 years, had for 3 months complained of pain and weakness in the left hip and leg. The conventional roentgen examination revealed an area of bone destruction in the pelvis close to the left acetabulum; the affected area was about as large as a child's palm and contained small portions of detached bone. Biopsy disclosed malignant tumour cells, probably from a hypernephroma metastasis.

Urography: The right kidney was normal in appearance and not displaced. The left kidney was situated in the midline of the true pelvis in front of the sacrum (Fig. 1). No obvious deformation of the renal pelvis was noted and for this reason and because the biopsy had suggested the presence of a hypernephroma, the patient was transferred to our department for renal angiography.

Renal angiography: This was carried out by percutaneous puncture of the right femoral artery and the insertion of a catheter. It was found that the pelvic kidney contained a rounded, richly vascularized hypernephroma with numerous pathologic vessels (Figs. 2 and 3). The kidney was supplied by two wide arteries arising approximately at the bifurcation of the aorta. Simultaneous contrast filling of a large number of tumour vessels with arteriovenous fistulae in the area of destruction in the pelvis and similar vessels in the surrounding soft parts was obtained. An extremely wide superior gluteal artery together with a widened superficial circumflex iliac artery contributed to the vascular supply of this region.

The patient died about a year after the examination and the roentgenologic findings were all confirmed at autopsy (Fig. 4).

Discussion

In agreement with the observations of CAMPBELL and BELL, I found from a survey of our material that the ectopic kidney often has an abnormal shape. The ureter of a pelvic kidney cannot as a rule be satisfactorily compressed and the renal pelvis will consequently be poorly filled. It is true that contrast filling of the renal pelvis may be obtained by means of pyelography but since the pelvis often has an anomalous shape, it is clear that this method of examination will generally also not prove satisfactory for a definite diagnosis of an expansive process in the kidney or the exclusion of such a lesion.

A normal renal pelvis on the other hand does not exclude the presence of a malignant tumour, as shown *e. g.* by OLHAGEN and LÖFGREN and in some measure demonstrated by the case now reported.

It will be clear from the above considerations that urography and retrograde pyelography offer only limited possibilities for excluding or demonstrating the presence of a renal tumour in a case of ectopic kidney as compared to cases with kidneys in normal positions. Despite the fact that a tumour in an ectopic kidney is uncommon it would appear from the ratios of frequency mentioned in the introduction that it is not quite so rare as might be imagined from the comparatively few cases published. The employment of renal angiography in all cases of renal ectopia appears to be an essential diagnostic procedure.

SUMMARY

A case of renal ectopia with hypernephroma diagnosed by means of renal angiography is described. It is stressed that this procedure is most desirable in the examination of cases of renal ectopia.

ZUSAMMENFASSUNG

Ein Fall von Nierenektopie mit Hypernephrom, welches durch eine renale Angiographie diagnostiziert worden ist, wird beschrieben. Es wird betont, dass diese Prozedur für die Untersuchung von Fällen mit renaler Ektopie am besten geeignet ist.

RÉSUMÉ

L'auteur présente un cas d'ectopie rénale avec cancer du rein diagnostiqué grâce à l'angiographie rénale. Il souligne le grand intérêt de cette technique pour l'examen des cas d'ectopie rénale.

REFERENCES

1. Baggenstoss, A. H.: Congenital anomalies of the kidney. Med. Clin. N. Amer. 35 (1951), 987.
2. Bartley, O. and Hultquist, G. T.: Spontaneous regression of hypernephromas. Acta path. microbiol. scand. 27 (1950), 448.
3. Bell, E. T.: Renal diseases, pp. 27, 432. Lea & Febiger, Philadelphia 1950.
4. Campbell, M. F.: Renal ectopy. J. Urol. 24 (1930), 187.
5. Earlam, M. S. S., Carrodus, A. L. and Howarth, V. S.: Unilateral renal ectopia with renal carcinoma. Aust. N. Z. J. Surg. 19 (1950), 291.
6. Langworthy, H. T. and Drexler, L. S.: Carcinoma in crossed renal ectopia. J. Urol. 47 (1942), 776.
7. Lee, H. P.: Cited by Earlam et coll.
8. Löfgren, F. O.: Renal tumour not demonstrable by urography but shown by renal angiography. Acta radiol. 42 (1954), 300.
9. Mc Kenzie, L. W. and Hawthorne, A. B.: Cited by Earlam et coll.
10. Olhagen, B.: Hypernefromdiagnos vid negativ urografi (Swedish), Svenska LäkT. 51 (1954), 7.
11. Patch, F. S.: Carcinoma in a crossed heterolateral ectopic kidney, without fusion. Brit. J. Urol. 9 (1937), 339.
12. Seldinger, S. I.: Catheter replacement of the needle in percutaneous arteriography. A new technique. Acta radiol. 39 (1953), 368.
13. Stevens, A. R.: Pelvic single kidneys. J. Urol. 37 (1937), 610.
14. Thomas, G. J. and Barton, J. C.: Ectopic pelvic kidney. J. A. M. A. 106 (1936), 197.
15. Ultzmann, H.: Karzinosarkom in gekreutzt dystoper Niere. Z. Urol. 46 (1953), 41.
16. Wulff: Carcinomatös entartete linkseitige Beckenniere. Dtsch. med. Wschr. 2 (1907), 1882.
17. Young: Cited by Earlam et coll.

FROM THE ROENTGEN DEPARTMENT (DIRECTOR: YRJÖ V. PAATERO), INSTITUTE OF DENTISTRY, UNIVERSITY OF HELSINKI, HELSINKI, FINLAND

PANTOMOGRAPHY OF SPHERICAL LAYERS

by

Yrjö V. Paatero

In earlier articles I have shown that it is possible with the pantomographic method to roentgenograph layers of nearly any form, and situated at any depth (2, 3, 4, 5). In practice, however, there are certain technical limitations; for instance, for the production of spherical layers, suitably shaped films are not obtainable. In my opinion, however, this disadvantage should not be a complete bar to solving the problem, especially since limited spherical layers, such as those of a bony cranium of sufficiently large radius, may be pantomographed with ordinary film. It should be pointed out that the greater the radius of a sphere or of a cranium, the less the spherical layer or surface differs from a plane and, furthermore, the greater the possibility of pantomographing small areas of the cranium with ordinary films. I shall return to this practical matter again after treating the problem theoretically.

If a spherical layer, such as the cranial vault, is to be examined, an apparatus called a pantomograph must be employed. This should be furnished with a rotating film holder (2, 4) because it is not possible to reproduce spherical layers in a film moving in a straight line (1, 3).

Let us now assume that there is a cylindrical object (*Obj.*) on the object holder (*Oh*) from which a thin layer (*S*), corresponding to a

Submitted for publication 25 January 1957.

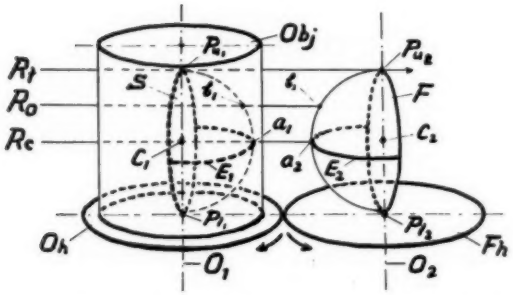

Fig. 1. Pantomography of spherical layers with spherical films.

hemisphere, is to be reproduced in a roentgen film (Fig. 1). In accordance with the principles of pantomography, a film (*F*), the form and location of which correspond to those of the layer to be roentgenographed, is placed on the film holder (*Fh*). For the sake of simplicity, both the layer *S* and the film *F* are positioned concentrically in relation to the rotation axes (O_1 and O_2) and, in addition, the narrow vertical roentgen beam directed from the left through the object (*Obj.*) to the film (*F*) consists of parallel rays. The central ray (*Rc*) penetrating the center (C_1) of the hemisphere (*S*) strikes the center (C_2) of the hemispheric film (*F*); hence this ray penetrates the layer (*S*) perpendicularly at point a_1, through which the equator (E_1) is drawn. The corresponding landmarks of the film (*F*) are a_2, and E_2. All points situated on the equator (E_1) will be projected onto the film at a right angle. Hence, the detail of the image will show up best on the equatorial circle (E_2).

The uppermost ray (*Rt*) passes the layer (*S*) and the film (*F*) tangentially at points Pu_1 and Pu_2, respectively. Detail will thus be poorest at point Pu_2; in fact, there cannot be any image of the object at the said point since point Pu_1 accomplishes merely a rotational movement on the axis (O_1). The situation is the same as far as the lowermost point (Pl_1) of the layer is concerned; its projection onto the film will be the point Pl_2.

Ro denotes an arbitrary ray between the former ones. It will always penetrate the layer (*S*) obliquely and reach the film obliquely, too. It may be seen from Fig. 1, that the nearer *Ro* is to *Rc*, the more vertical the tangential planes of the said spherical layers will be at points b_1 and b_2 and accordingly, the clearer the respective circle of latitude will be projected onto the film. We may conclude that the central ray *Rc* produces the maximum detail and the tangential ray (*Rt*) the minimum. This applies also to the lower half of the hemisphere.

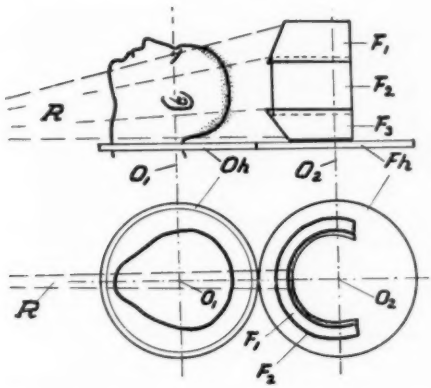

Fig. 2. Pantomography of spherical layers with ordinary films.

In practice, the nature and projection of the rays must vary with the examination. For instance, if it is the question of examining a fracture the roentgen rays may penetrate the bone more obliquely than when other changes are to be studied. In any case, if spherical films and intensifying screens were available, it would also be possible to roentgenograph spherical layers. Many of the cranial bones, because of their rounded shape, would be particularly suitable for reproduction. It is clear that the films cannot be flattened but, in spite of their needing more space than ordinary films, can be filed as they are.

It should be pointed out that it is not necessary to position the layer to be roentgenographed and the film concentrically. This is quite impossible in many cases, as, for instance, when the spherical layer is not regular. In any case, the form and position of the film determine the layer of the object to be reproduced. If several layers are to be examined simultaneously, an equal number of films should be placed on the rotating film holder. The size, form, and situation of the films may, if necessary also be different. For instance, one film might be flat in its vertical plane but bent or flat in its horizontal dimension, the second film conical, the third spherical, etc.

For the sake of simplicity, it was assumed in the foregoing that the roentgen beam consisted of parallel rays. This means, in practice that the source of the rays, the focus, is situated at infinity. The focal spot of the roentgen tube will, however, be rather close to the object and film and hence a so-called divergence correction in the location and shaping of the film must be made as explained previously (2). Furthermore, because the rays diverge from the focus, the tangential rays of

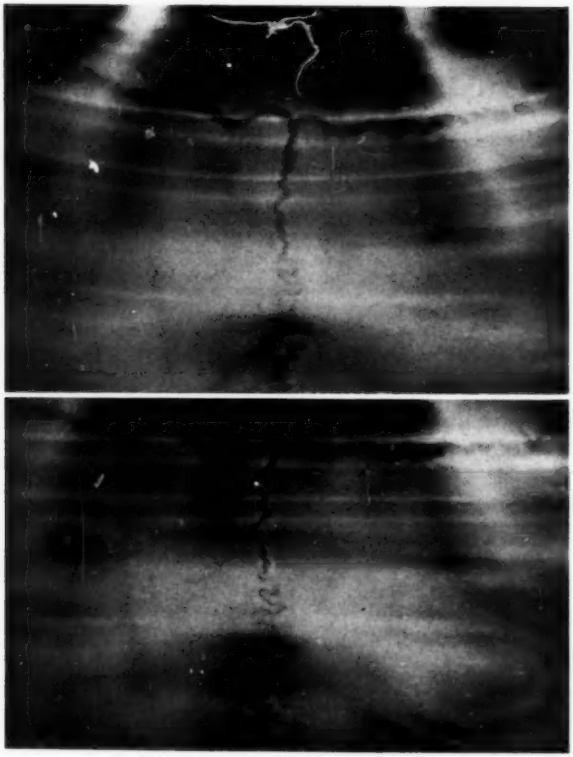

Figs. 3 and 4. Pantomograms of the vault of a human dry skull taken with ordinary films bent to shape.

the roentgen beam cannot pass the film at the uppermost point (Pu_2) and the lowermost point (Pl_2), but they will do so somewhere between the said points and the equatorial point (a_2). The direction of all other rays in this case is correspondingly more oblique in relation to the surface of the film. This means, that the diagnostically useful region is now smaller vertically than if the rays were parallel. The closer the focus to the object, the narrower is the "band" that can be produced clearly in the film, and vice versa. In practice, however, even the surface of an entire sphere may be pantomographed since it is possible to make several exposures and turn the object between them. By these means the whole human skull could be reproduced in two or three spherical films, although if necessary a larger number of films, either of ordinary shape or cut to the form of the skull might be employed.

Fig. 5. Pantomogram of the vault of a human dry skull taken with ordinary film bent to shape.

For the stereoscopic examination of spherical and similar layers, tridimensional pantomograms may be obtained, although the area to be seen stereoscopically at one time is very limited. In this case the same factors previously presented in my article on stereoscopy of conical surfaces (5) apply because in effect the spherical surface consists of numerous small, conical band-like surfaces. In addition, the observer is able to see only a very limited area of the spherical film facing him. If the whole sphere or a larger area of it is to be observed it must be turned round like a map globe and one area after another studied. A source of light should, of course, be situated within the spherical film when it is examined.

Since one may regard the spherical layer or surface as built up of numerous narrow conical and single band-like surfaces, it will also be possible to roentgenograph the spherical layer upon similar films. In practice, however, the use of many separate films is too complicated and three films may conveniently be used when the whole of the cranial vault is pantomographed. One such procedure is shown schematically in Fig. 2. The patient's neck is within the object holder (neck ring) (*Oh*) with the head tilted backwards. Three films in flexible cassettes are on the film holder (*Fh*). The top film (F_1) and the bottom film (F_3) are conical; between them is a vertical film bent horizontally (F_2). It will be noted that the superior part of the vault will be projected onto the upper conical film, the middle part onto the vertical film and the inferior part onto the lower conical film. The roentgen beam (*R*) consists of diverging rays, as is usual in practice. Accordingly the shape and the situation of the films are somewhat different for the divergence correction than the location of the layer to be reproduced. This problem I have treated in detail in a recent paper (2).

I should like to point out that it is not necessary to locate the head and films as in the illustration. The source of the roentgen rays may also be higher or lower. The dotted area in Fig. 2 denotes approximately the thickness of the layer which will be seen in the films. Because the bone tissue in this case is rather thin, the whole of it will appear in the pantomogram.

It is of course possible, and in certain cases even advantageous, to pantomograph the various areas of the vault of the cranium separately; the skull may be moved between the exposures and, if necessary the roentgen tube may be lowered or raised. The form of the head and the diagnostic purpose determine the positioning and the best projection.

Three pantomograms of the vault of a dry skull are shown in Figs. 3, 4, and 5. In order to simulate live conditions, a rubber bag filled with water was introduced into the skull. The pantomograms in Figs. 3 and 4 were obtained with a single exposure and with the skull positioned as in Fig. 2. The films were ordinary flat films measuring 13 by 18 cm but bent as in Fig. 2, the top one conically and the second horizontally.

Before the pantomogram shown in Fig. 5 was taken the skull was placed in the mento-frontal position, the Frankfurt plane being horizontally. The roentgen beam thus penetrated the facial part of the skull before reaching the posterior part of the vault and the film. The film was not conical in this case but vertical and bent horizontally to correspond approximately to the posterior part of the skull. If the resulting pantomogram is studied it will be noted that there are no traces of the facial bones; only blurred lines are seen, caused by the part of the vault and other bony structures which were not located at the same distance from the rotational axis as the corresponding points of the film. It is to be expected that only a very limited area of the vault can be sharply reproduced; an ordinary film cannot follow the shape of the spherical bone. For each exposure the outermost part of the object to be roentgenographed was located about 11 cm from the rotational axis, and the film a corresponding distance from its own axis.

Both the theoretical and experimental part of this study in my opinion shows that it is possible to reproduce spherical and comparable surfaces on film with the pantomographic method. Since no spherical films are as yet available, ordinary roentgen films may be used, and by bending them suitably it is possible to obtain quite useful pantomograms of limited areas of spherical layers.

This paper has been confined to pantomography of the skull. There are however, other parts of the human body which may be suitable for spherical pantomography.

SUMMARY

Investigations have shown that it is possible to obtain pantomograms of spherical and similar layers. The films should also be spherical, but within certain limits quite good results may be obtained with ordinary films, provided the radius of the layer is not too small and the area of the layer is not large. In using ordinary flat films, they may be bent to correspond approximately to the limited area of the spherical layer to be examined. The pantomograph must be furnished with a film holder capable of being rotated, particularly if spherical films are used.

ZUSAMMENFASSUNG

Untersuchungen haben die Möglichkeit aufgezeigt, Pantomogramme sphärischer und ähnlicher Schichten herzustellen. Die Filme sollten ebenfalls sphärisch sein, aber innerhalb gewisser Grenzen können recht gute Resultate mit gewöhnlichen Filmen erreicht werden, vorausgesetzt dass der Radius der Schicht nicht zu klein und die Flächenausdehnung der Schicht nicht zu gross ist. Bei Benutzung gewöhnlicher Planfilme können diese so gebeugt werden, dass sie ungefähr dem Gebiet der zu untersuchenden sphärischen Schicht entsprechen. Der Pantomograph muss mit einem rotierbaren Filmhalter ausgerüstet sein, besonders wenn sphärische Filme benutzt werden.

RÉSUMÉ

Une étude expérimentale a montré qu'il est possible d'obtenir des pantomographies de couches sphériques et analogues. Il faudrait que les films aussi soient sphériques, mais, dans certaines limites, on peut obtenir de très bons résultats avec des films ordinaires, à condition que le rayon de la couche de coupe ne soit pas trop petit et que sa surface ne soit pas trop grande. Il est possible d'incurver des films plans ordinaires de façon à les faire correspondre approximativement à la surface limitée de la couche sphérique à examiner. Le pantomographe doit être pourvu d'un porte-film capable de tourner, en particulier quand on utilise des films sphériques.

REFERENCES

1. Paatero, Yrjö V.: A new tomographical method for radiographing curved outer surfaces. Acta radiol. 32 (1949), 177.
2. — Pantomography in theory and use. Acta radiol. 41 (1954), 321.
3. — The principles of the construction and function of the stereo-pantomograph. Acta radiol. 43 (1955), 113.
4. — Die Anwendung der Pantomographie für klinische Untersuchungen. Fortschr. Röntgenstr. 82 (1955), 525.
5. — Kartiopintojen muodoista stereopantomografiassa. (Finnish.) Suom. hammaslääk. toim. 52 (1956), 145. (Studies on the shape of conical surfaces in stereopantomography.) (To appear in Acta odont. scand.)

FROM THE DEPARTMENT OF RADIOLOGY (DIRECTOR: PROF. C. WEGELIUS),
UNIVERSITY OF TURKU, TURKU, FINLAND

SEGMENTAL ROENTGENOGRAPHY BY MEANS OF A STANDARD TOMOGRAPHIC DEVICE

Preliminary report

by

Pekka Vuorinen

Roentgenographic procedures utilizing a narrow beam of radiation and movement of the tube, object and/or film, have been described by ALBERS-SCHÖNBERG (1906), MILLWEE (1937), HECKMANN (1939), PAATERO (1948), SCHALTENBRAND (1953), and JOHANSON (1956), inter alios.

This communication describes a procedure for roentgenography based on a narrow beam exposure with movement of only the tube with the object and the film stationary. This arrangement is easily achieved, without any complicated additional apparatus, by utilizing the tube portion of any tomograph.

The film is not placed in the coupled mobile cassette holder, but on the same side of the object in contact with the patient — in practice in a standard cassette between the body and the stand. The tube window is covered by a lead shield with a narrow slit transverse to the direction of the tube movement. On exposure, the slit allows only a narrow beam of radiation to pass through the object. The tube moves through the same angle with the same motion and speed as in conventional tomography.

Submitted for publication 6 april 1957.

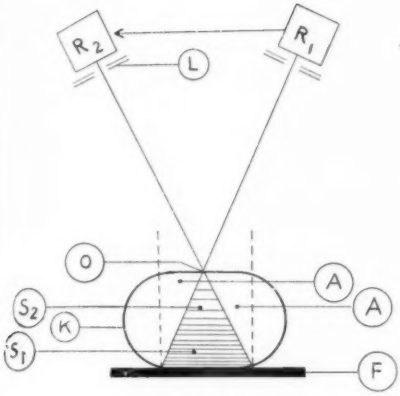

Fig. 1.

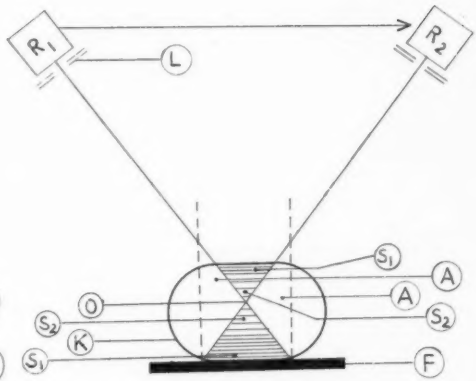

Fig. 2.

Fig. 1. Projection conditions. R_1—R_2 = movement of roentgen tube during exposure. L = lead shield with narrow slit transverse to tube movement at tube opening. O = center of axis of tube movement. K = object. F = film. A = parts of object remaining outside projection. S_1 = layers which are distinctly recorded. S_2 = layers which by blurring are indistinctly recorded.

Fig. 2. Various projection conditions. Legends as in Fig. 1. Axis of tube movement, O, situated at middle of object.

Geometric positioning of the axis of the tube movement in relation to the object results in a restricted segmental projection in the film. The conditions are demonstrated in Fig. 1, in which linear movements of the tube are shown. An arrangement with the axis of this movement kept at the tube side of the object appears to be satisfactory, as far as we can judge by the preliminary results. Fig. 2. demonstrates a variation of the positioning of the object to the moving roentgen beam, in which the axis lies at the centre of the object.

An analysis of the conditions for projection and representation in the film produces the following facts. If the slit at the tube opening is extremely narrow and the roentgen beam consequently exceedingly thin, *i. e.* a plane, which in practice is impossible, all the elements within the margins of the segmental borderlines will be clearly reproduced. As the beam plane, however, has a certain thickness and the tube is moving, the result is a poor or completely blurred representation of the elements close to the axis of movement. In Figs. 1 and 2, the axis is indicated by the point O. The nearer to this the parts of the object are, the wider they become dispersed in the film and, as a result both of over-exposure and motion unsharpness, they are totally obscured. At the same time, a clear representation of ele-

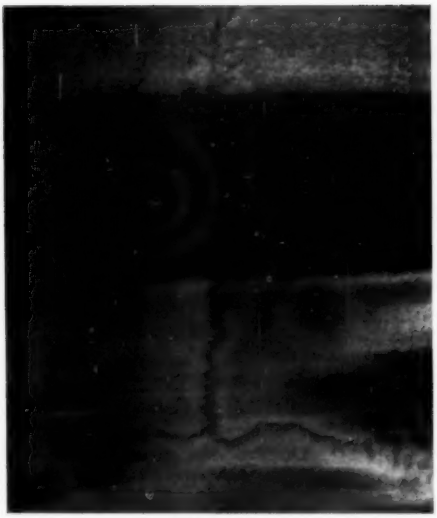

Fig. 3.

Fig. 4.

Fig. 3. Demonstration without superimposed shadows of the coronal and sagittal sutures of a dried cranium by means of 'segmentography'. The foramen magnum, close to the movement axis, is blurred out as a dark broad band-shaped shadow, and does not obscure the detail.

Fig. 4. Anterior portions of first ribs and the medial parts of clavicles. Posterior parts of ribs blurred out. Axis in region of bodies of thoracic vertebrae. Tube movement identical with longitudinal body axis.

ments far from the axial point but close to the film, is favoured. The shorter this distance is, the more distinct is the reproduction, and free from superposition of detail from more distant parts. The final result is very much the same as that obtained by means of conventional tomography — a clear visualization of certain layers, *i. e.* the layers closest to the film (Fig. 1). The procedure, however, differs from tomography principally in the very important respect that all the elements outside the segment (A in Figs. 1 and 2) are eliminated from the recordings. In tomography the parts of the object other than the layer to be examined are blurred out during the exposure.

A further advantage of 'segmentography' is the proportionally low irradiation dosage administered to the patient, by reason of the use of only a narrow beam of roentgen rays. It was calculated that the total amount of irradiation received was about the same as was to be expected in ordinary roentgenography of the same object, although the geometric distribution of the dose was different. In the closest related procedure in which a narrow beam (HECKMANN) is employed the object is completely irradiated during the whole exposure and consequently the dosage is considerably higher.

The procedure is illustrated by the roentgenograms in Figs. 3 to 6, the first being of a dried skull and the others of normal parts in living subjects. The films show the successful elimination of any shadows likely to be

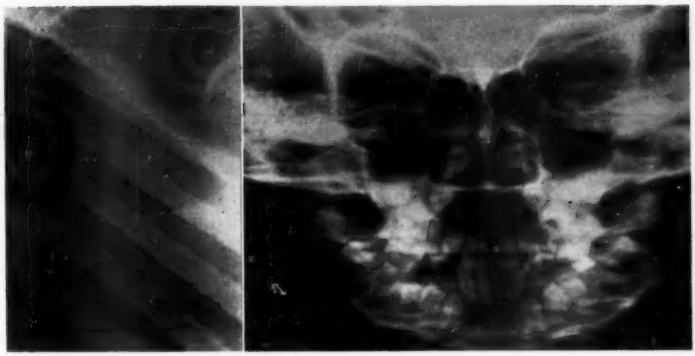

Fig. 5. Fig. 6.

Fig. 5. Posterior parts of upper ribs with anterior portions blurred out. Exposure data same as in Fig. 3. Film posterior and axis anterior to thorax.

Fig. 6. Facial bones of child, aged 8. Structure not obscured by superimposed occipital parts of skull. Film anterior with movement axis in occipital region.

superimposed from behind. A Siemens planigraph with linear movement of the tube was used, the cassette being in contact with the patient. The slit used was 1 mm.

This presentation is of a preliminary nature and does not claim to be a complete study. The choice of the optimal geometric conditions for a given layer is being closely examined and the results will be reported. The employment of a standard tomographic apparatus for the procedure may facilitate its practical application and establish its diagnostic value.

SUMMARY

A method of performing segmental roentgenography by means of a moving tube and fixed object and film is described. It may be used with any tomograph and no additional apparatus is necessary.

ZUSAMMENFASSUNG

Eine Methode zur Ausführung segmentaler Röntgenuntersuchungen mit Hilfe einer beweglichen Röntgenröhre und fixierten Objekt und Film wird beschrieben. Sie kann bei jeder Tomograph benutzt werden; zusätzliche Apparate sind nicht notwendig.

RÉSUMÉ

L'auteur décrit une méthode de radiographie segmentaire au moyen d'un tube en déplacement, l'objet et le film restant fixes. Elle peut être utilisée avec n'importe quel tomographe et ne nécessite pas d'appareil supplémentaire.

REFERENCES

Albers-Schönberg, H. E.: Röntgentechnik. 6. Aufl. Bd. 1, S. 284. Georg Thieme, Leipzig (1906) 1941.

Groedels, F. M.: Lehrbuch und Atlas der Röntgendiagnostik in der inneren Medizin und ihren Grenzgebieten. Bd. 1, S. 56. J. F. Lehmanns Verlag, München 1934.

Heckmann, K.: Die Röntgenperspektive und ihre Umwandlung durch eine neue Aufnahmetechnik. Fortschr. Röntgenstr. 60 (1939), 114.

Johanson, C. E.: Radiology in obstetrics. Acta obstet. gynec. scand. 35 (1956), 215.

Millwee, R. H.: Slit scanography. Radiology 28 (1937), 483.

Paatero, Y. V.: The use of mobile source of light in radiography. Acta radiol. 29 (1948), 221.

— Pantomography in theory and use. Acta radiol. 41 (1954), 321.

Schaltenbrand, G.: Orthoroentgenography. Am. J. Roentgenol. 70 (1953), 114.

FROM THE DEPARTMENT OF RADIOTHERAPY (DIRECTOR: B. EBENIUS) AND DEPARTMENT OF OPHTHALMOLOGY (DIRECTOR: PROFESSOR S. LARSSON), UNIVERSITY HOSPITAL OF LUND, SWEDEN

RADIATION THERAPY IN VERNAL CONJUNCTIVITIS

by

Bertil Ebenius, Sven Larsson, Ebbe Cederquist, and *John Cristiansson*

Radiotherapy is as a rule not resorted to in the treatment of mild vernal conjunctivitis. In the management of severe forms of the condition, however, radiotherapy has been used for more than 50 years — roentgen therapy since 1903 and radium since 1906. The literature on this subject is now fairly extensive, but most papers do not give the necessary physical data on the radiation or more detailed information on the technique and the dosage employed, which often makes it impossible to judge the results in relation to other methods of treatment and dosage.

In view of the divergence of opinion on the value of radiation therapy in vernal conjunctivitis we started the present investigation, the purpose of which was to judge the various possibilities of radiotherapy from an ophthalmologic as well as a radiologic point of view, in order to elucidate the requirements for a favourable result in the treatment of the tarsal and the limbal changes.

Methods of Radiotherapy

From a therapeutic point of view the tarsal and the limbal changes should be dealt with separately because of their difference in nature and relation to surrounding tissues.

Submitted for publication 4 May 1957.

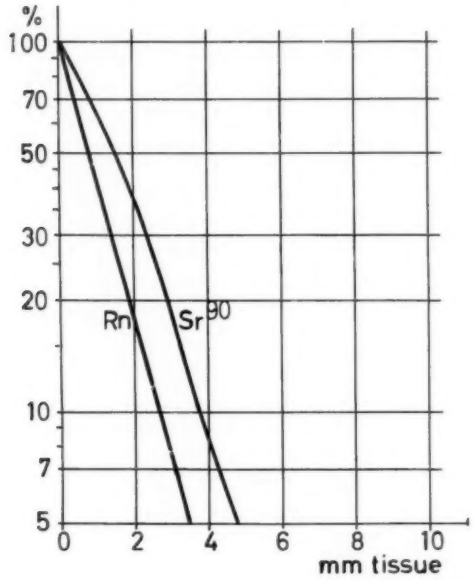

Diagram 1. Depth dose curves for our radon and Sr^{90} applicators.

TARSAL CHANGES

Vernal excrescences seldom protrude more than 1 to 2 mm; in the irradiation of these excrescences with the eye-lid averted it is therefore of importance that the major portion of the radiation reaches this depth without, however, involving the deeper healthy tissue more than is necessary. In the treatment of tarsal changes, then, the power of penetration of the rays should be relatively small. These theoretical requirements can be satisfied by beta radiation from radioactive substances and by soft roentgen rays, both of which have been used for vernal conjunctivitis.

Treatment with beta radiation

Radium, radon, radium D. In order effectively to utilise beta radiation from radium, the applicator must be provided with a filter permitting the passage of the major portion of these rays. Several types of applicators have been described (ILIFF, 1947, LEDERMAN 1947, HAGUE 1952) but the disadvantages of unavoidable gamma radiation, for example, has limited their use.

The radon gas is usually kept in a glass container (BURNAM and NEILL 1940 and ILIFF 1951) and if the wall of the container is thin, a very high in-

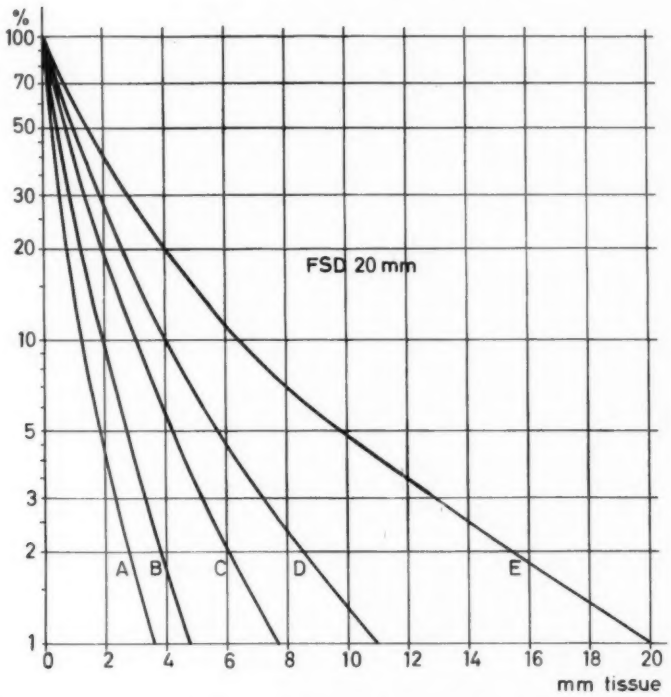

Diagram 2. Depth dose curves for soft roentgen rays. FSD = 20 mm.
A = 10 kV, 0 filter added
B = 10 kV, 0.05 mm Al
C = 15 kV, 0.05 mm Al
D = 20 kV, 0.10 mm Al
E = 30 kV, 0.25 mm Al

tensity of radiation may be obtained. In view of the difficulty in obtaining a glass wall of uniform thickness applicators otherwise equal can give beta radiation of widely varying intensity and quality, which thus makes it difficult to control the dosage. A considerable disadvantage in the use of radon is that the gamma radiation cannot be eliminated. When the intensity of the beta radiation is high in relation to that of the gamma radiation, the effect of the latter on the lens of the patient and on other radiosensitive tissues will be relatively small. On the other hand, it is difficult to protect the members of the staff sufficiently without special precautions. It appears that this has not received sufficient attention, although the hazards of such radiation have been pointed out (PENDERGRASS and ANDREWS 1935, FRICKE 1951).

The doses received by the staff of the department of radiotherapy, Lund, during the radon treatment were studied. It was found that in the beginning the operators manipulating the applicators were exposed — mainly because of the gamma rays — to more than the maximum permissible body doses. By the employment of a protective shield the exposure to radiation was markedly reduced (CEDERLUND, LIDÉN and LINDGREN 1957) and demonstrated the importance of protection in radon treatments.

The surface to be irradiated in the treatment of the tarsal changes is fairly large. If the dose is to be spread equally over the entire field, applicators of a diameter as small as 4 to 5 mm should not be used because they must be moved to and fro throughout the treatment. In this so-called spray method the dose will be uneven and involve a risk of overdosage and underdosage in certain regions.

Another product of the disintegration of radium, radium D, emits practically no gamma rays, the effect therefore being ascribable only to beta rays. Because of its low energy, however, the effect of most of the beta particles from radium D is not deep enough to influence the tarsal changes.

Radioactive isotopes. Radioactive phosphorus has been tried clinically in the treatment of vernal conjunctivitis, but owing to the low intensity of the beta radiation from P^{32}, it cannot be used with advantage. Its employment is accompanied by other disadvantages such as the relatively short half-life and the risk of fragmentation and consequent contamination with lacrimal fluid (LEDERMAN 1956). On the other hand, irradiation with radioactive strontium (Sr^{90}) has been found to produce favourable results (FRIEDELL, THOMAS, and KROHMER 1955). Applicators of high intensity, suitable for short manual application, are now available. These applicators may be used with advantage in the treatment of superficial changes, provided that they are of suitable design with a surface preferably large enough to permit treatment of the entire region at a time.

In the use of such applicators with radioactive substances the choice of treatment must be dictated by the spread of the changes on the surface and their height. The power of penetration of beta rays is limited (Diagram 1). In the treatment of high excrescences on the inside of the eye-lid it is therefore hardly possible to obtain a satisfactory effect on the deepest part of the excrescences without simultaneous overdosage on the surface.

Roentgen treatment

Treatment with conventional apparatuses with medium hard rays (60 — 100 — 200 kV) is often given as a 'whole eye technique' in small fractionated doses (LEDERMAN 1952). In order to avoid cataract the total dose must be kept so low that, in our opinion, it will scarcely have sufficient effect on the vernal changes.

Contact roentgen therapy is more suitable, both on theoretical grounds and in practice. Apparatus for this type of treatment is now available with a voltage that can be varied from 50 or 60 kV to 10 kV to produce soft to extra-soft radiation; a suitable filter is selected for the penetration required (Diagram 2). The method permits homogeneous irradiation of the entire inner side of the eye-lid and at the same time the eye-bulb can be protected. It thus satisfies all the theoretical requirements for a suitable surface therapy of the palpebral changes in vernal conjunctivitis.

LIMBAL CHANGES

The radiologic treatment of the limbal changes in vernal conjunctivitis should preferably follow the same principles as the treatment of the tarsal changes. It must be remembered, however, that the limbal changes are often much thinner than the tarsal, and still greater consideration must be given to the depth dose in relation to the proximity of the lens and ciliary body. The distance between the limbus and the equator of the lens is, according to VON SALLMAN, 2.5 to 3.3 mm. The thickness of the cornea at the limbus is usually given at 1.2 to 1.4 mm; the distance between the limbus and the ciliary body is only 1.5 to 2 mm. The quality of the radiation selected should therefore be such that the energy emitted is absorbed mainly in a tissue layer corresponding to the thickness of the vernal changes.

The same sources of radiation considered suitable for the treatment of the tarsal changes have also been used for the limbal changes. But not all fill the above requirements.

Beta radiation from radium and radon has satisfactory penetrating power but the unavoidable gamma radiation makes these two substances less suitable. It is above all the risk of cataract that must be taken into account. In irradiation of the region of the limbus with radon applicators, MERRIAM 1955, observed cataract in 8 cases out of 10 after a calculated focal dose of 230 to 1,100 rep at a depth of 3 mm. But the smallest dose produced only 'stationary opacity'. Radium D is in this respect better because the gamma radiation is negligible. Its beta radiation has, however, such small penetrating effect that RaD can only be used in the treatment of thin superficial changes. The activity of available sources is low, which therefore makes the time of treatment long.

Strontium^{90} is better as a source of beta radiation, but it is questionable whether all strontium applicators are suitable for the treatment of the limbal changes in vernal conjunctivitis. The relative depth doses of some applicators are fairly high, about 18 per cent (SINCLAIR and TROTT 1956) and 15 per cent (VON SALLMAN, MUNOZ and DRUNGIS 1953) at a depth of 3 mm, but even when using applicators with a relative depth dose of 7

UNIVERSITY OF MICHIGAN LIBRARIES

per cent (HAGUE) and 9 per cent (FRIEDELL et coll. 1955) at 3 mm depth the risk of cataract should be borne in mind. Judging by our experience, relatively large doses are necessary to produce a satisfactory effect on the vernal changes.

Experimental investigations (VON SALLMAN et coll. 1953, MACDONALD, HUGHES, and PFEIFFER 1955) with irradiation of the region of the limbus of the rabbit have shown that relatively small doses can produce cataract. VON SALLMAN, for example, states that a surface dose of 5,000 rep (15.5 per cent at 3 mm depth) from Sr^{90} applicators can produce cataract in the rabbit and MACDONALD et coll. maintain that it can be produced by a minimum dose of 500 to 1,000 rep (12 per cent at 3 mm depth). The germinative zone of the lens of the rabbit is, however, much more sensitive than that in man. FRIEDELL et coll. never observed lenticular opacities after having used Sr^{90} applicators for 4 years, but they pointed out that the follow-up was too short to permit any valid conclusions. In the treatment of limbal changes they applied at most 9,600 and at least 3,250 rep in surface doses; if the changes do not respond to moderate doses they recommend some other type of therapy. In the use of large surface doses the risks of untoward effects on the cornea, conjunctiva, sclera, and uvea should also be considered (MERRIAM 1956).

We have no personal experience with the use of strontium-applicators in the treatment of vernalis changes. In other changes in the cornea we have, however, employed strontium ^{90} contact shells (described by SINCLAIR and TROTT, LEDERMAN 1956). After the hitherto largest surface dose of 5,000 rep for 4 weeks we have observed no complications during a follow-up of 1.5 years which is, however, not long enough to permit any evaluation of late radiation changes.

Contact roentgen therapy. What was said above concerning this therapy holds also for irradiation of the limbus. Thanks to the possibility of adjusting the penetrating power of the rays by a suitable choice of voltage, filter, and treatment distance, the conditions necessary for sparing the lens and the ciliary body can be satisfied. The use of roentgen apparatus for contact therapy for limbal changes can be facilitated by certain technical arrangements.

Own material

The material comprised 11 cases (20 eyes) of vernal conjunctivitis treated during the years 1944—1951.

Clinical findings

Most of the patients had a long history of severe symptoms that had been refractory to earlier treatment (Table 1). In 9 of the patients both

Table 1

Survey of material

Case No.	Age in years and sex ♂	Age in years and sex ♀	Duration of symptoms in years	Tarsal lesions	Limbal lesions	Earlier treatment
1	23		12	R L		Antihistamine + vasoconstrictor
2	27		11	R L	L	Antihistamine + vasoconstrictor
3	34		10	R L		Excision
4	12		2	R L		Antihistamine + vasoconstrictor
5	13		3/12	R		Unspecific desensitization
6	9		3	R L		Antihistamine + cortisone
7	14		3	R L		Cortisone
8	15		8	R L		Unspecific desensitization. Corrosion. Cortisone
9		12	6	R L		Antihistamine
10	20		10	R L		Antihistamine
11		35	11	L	L (cornea)	Unspecific desensitization. Antihistamine. Electrocoagulation. Excision + transplantation of lip mucosa.

eyes were involved. Nine had only tarsal changes, the remaining 2 limbo-corneal changes as well.

The symptoms were those usually experienced in this condition: a burning sensation, the feeling of a foreign body, photophobia, itching, lacrimation and a sticky conjunctival secretion.

The examination revealed diffuse general hyperplasia of the tissue of the tarsal conjunctiva, with the formation of separate, small or large, vegetation, in advanced cases flattened, compatible with the classical comparison with a 'cobblestone pavement'. There was usually slight ptosis and a stringy secretion, which could be pulled out of the fornix in long threadlike formations. In cases in which the limbus cornea was also involved, and the changes thus encroached upon the bulb, the conjunctiva was thickened with solitary nodules at the limbus, sometimes confluent, forming more extensive vegetations.

Case 11. The changes and the course of the disease in this case were so remarkable that they merit a more detailed description. A 48-year-old woman had a 12 years' history, the condition being practically unilateral. In addition to the characteristic but not advanced changes in the tarsus there was a tumour-like formation in the limbus (Colour Plate 5). This formation gradually increased in size. Histologic examination showed hyperplasia of the stroma, increased connective tissue, numerous round cells, and eosinophilic cells — a typical allergic reaction of the tissue. The picture thus coincided with that of vernal conjunctivitis.

Radiotherapy

The tarsal changes were treated with radon or by contact roentgen therapy.

Radon therapy was used for 4 eyes with tarsal changes. For reasons

Table 2

Radon treatment

Case No.	Region irradiated		Total surface dose [1]	Follow-up in years	Re-examination 1955		
	Tarsus	Limbus			Subj.	Vernalis lesions	Radiation reactions
1	L		Per 1 field: 2,500 rep/41 d.[2]	5	0	0	Atrophy, teleangiectases
2	L		Per 1 field: 2,500 rep/41 d.[2]	5	Feeling of foreign body	0	Atrophy, teleangiectases
		L	Per each of 2 fields 5,000 rep in single dose	5	Feeling of foreign body	0	Peripheral lenticular opacities
9	R		Per each 3 fields 16,500 rep/105 d.	3½	0	0	Atrophy teleangiectases
10	L		Per each of 3 fields 16,500 rep/77 d.	3½	Slight itching Slight feeling of foreign body	0	Atrophy, teleangiectases
11		L (cornea)	Per each of 4 fields 16,500 rep/190 d. 18,000 rep/97 d. 22,000 rep/85 d. 13,000 rep/70 d.	5	0	0	Teleangiectases

[1] Doses calculated according to measurements made at our Physics Department (S. HAGSGÅRD).
[2] Also contact roentgen therapy.

given above, dosage causes certain difficulties. In Cases 9 and 10 the doses were about 2,200 rep per field per treatment given at intervals of about two weeks. The total doses are included in Table 2. In Cases 1 and 2 it proved necessary to use the less reliable so-called spray method because of the disproportion between the surface of the applicator (about 12.5 mm²) and the fairly wide spread of the tarsal changes. The total doses calculated as approximately 2,500 rep/41 days, proved insufficient and further treatment was therefore given with contact roentgen therapy.

Contact roentgen therapy was used for the remaining eyes.

After averting the eye-lid the entire changed region was treated with an applicator 20 to 25 mm in diameter. The ciliary margin was spared and the bulb was protected with a rubber-lined lead spatula. Data: 50 kV. 2 mA, 0.2 mm Al filter, HVL 0.32 mm Al, FSD 18 or 38 mm. As a rule a single dose of 1,000 r was delivered every second week up to 4,000, 5,000 or 6,000 r. When this dose failed to produce healing, a further dose of 1,000 r was given once or twice after 2 months or more. Sixteen eyes were treated in this way only (Table 3).

The limbal changes were irradiated with radon only (Table 2). Two eyes required treatment. In Case 2 the patient received a single treatment

Table 8

Contact roentgen therapy

Case No.	Tarsus	Total surface dose	Follow-up in years	Re-examination 1955		
				Subj.	Vernalis lesions	Radiation reactions [2]
1	R	5,000 r/62 d.	5	0	0	+
	L	3,000 r/31 d.[1]	5	0	0	+
2	R	6,000 r/5 m. 2 series	5	0	Slight discharge	+
	L	4,000 r/42 d.[1]	5	Feeling of foreign body	0	+
3	R	9,000 r/10 m. 2 series	5	Slight photophobia	0	+
	L	7,000 r/85 d. 1 series	5	Slight photophobia	0	+
4	R	7,000 r/6 m.	4½	0	0	+
	L	7,000 r/6 m.	4½	0	0	+
5	R	6,000 r/70 d.	4½	Slight photophobia Slight itching	0	0
6	R	7,500 r/11 m. 2 series	3	0	0	+
	L	7,500 r/11 m. 2 series	3	0	0	+
7	R	3,000 r/30 d.	4	0	0	0
	L	5,000 r/72 d.	4	0	0	0
8	R	5,000 r/56 d.	4	Slight itching	0	+
	L	5 000 r/55 d.	2	Slight itching	Slight stringy discharge	+
9	L	5,000 r/63 d.	3½	0	0	+
10	R	4,000 r/49 d.	3½	Slight itching. Slight feeling of foreign body	0	+
11	L	8,000 r/98 d. 2 series	11	0	0	++

[1] Also radon treatment.
[2] + and ++ indicate mild and moderate atrophy and teleangiectases.

of 2 adjacent fields. In Case 11, with wide-spread and tumour-like changes, three stationary fields were used, in addition to which dilated vessels were treated by the 'spray method' in an area of 8 × 8 mm. The applicator was passed as uniformly as possible over the entire region to be treated and was kept in contact with the surface of the lesion throughout.

Results

A preliminary report on the results of this treatment was given by LARSSON (1952—53).

Judging by the objective findings made at reexamination (February—May 1955), of the total of 20 eyes treated, 18 had recovered completely from vernal conjunctivitis (Tables 2 and 3). The patients had been followed up for 2 to 11 years. In 2 eyes a slight amount of stringy secretion from the conjunctiva was noted (Cases 2 and 8).

Of the total number of patients, 5 had recovered both subjectively and objectively. Three had had very mild symptoms during certain periods of the year. None of them, however, showed any visible vernal changes. The 2 patients with persistent stringy secretion reported slight symptoms of conjunctivitis vernalis. In Case 11 (Colour Plate 5 a and b) the symptoms disappeared completely although the patient had had moderate tarsal and severe limbocorneal vernalis changes from the beginning. These had also disappeared, but a persistent moderately dense macula with a few isolated tortous vessels was present in the cornea. These opacities which permitted vision of 0.3 were such that they could probably be ascribed to earlier electrocoagulation. The conjunctivitis vernalis had thus healed.

Radiation changes seen on reexamination were usually so mild as not to produce symptoms. Late macroscopic palpebral radiation reactions appeared almost regularly as fine ectatic vessels on the tarsus and mild mucosal atrophy. Only with difficulty could both teleangiectases and atrophy of the tarsus be detected with the naked eye, excepting in Case 11. But in this case the dose had been remarkably large. No temporary or permanent loss of cilia was observed.

In Case 2, where the limbus was irradiated with radon, a peripheral cataract was noted with small cystic opacities in that part of the equator corresponding to the treated limbus sector. It is possible that overlapping occurred. The opacities were, however, so limited that even 5 years after radiation treatment they had not produced any visual disturbances.

Conclusions

The investigation thus showed that even severe forms of conjunctivitis vernalis respond favourably to radiotherapy (Colour Plate 1—5). The doses must, however, be fairly large. If the first series of treatment does not produce the desired result, a second treatment is recommended — though not until after an interval of 2 months.

The material is too small to permit any definite conclusions on the relative value of radon treatment and contact roentgen therapy, but the results obtained appear to be roughly equal.

1 a.

1 b.

2 a.

2 b.

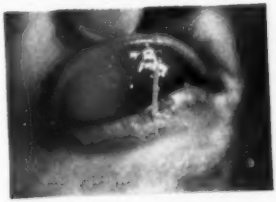

3 a.

3 b.

4 a.

4 b.

5 a

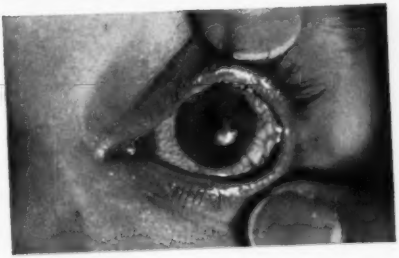

5 b.

Contact roentgen therapy in this material was used only for the tarsal changes because at that time we only possessed a 50 kV apparatus. We now have an apparatus with a voltage of 10 to 15 kV, with a beryllium window, and with this it is possible to choose a radiation of such low penetrating power as to minimize the risk of cellular injury in the equator of the lens and the ciliary body. The depth dose curves (Diagram 2) noted for this apparatus were much more favourable than those given for our strontium applicators (Diagram 1). It therefore appears that roentgen contact therapy given with suitable voltage, filter and distance might involve less risk also in the treatment of the limbal changes. The fractionation used with one treatment every other week proved advantageous, because as a rule it did not increase the symptoms by producing radiation reactions. As to the doses for contact roentgen therapy those mentioned appear to be suitable.

SUMMARY

The material consists of 20 eyes (11 cases) of vernal conjunctivitis treated with radon and contact roentgen therapy, and which were followed up for 2 to 11 years. Eighteen recovered completely and 2 were considerably improved. The two forms of therapy are discussed. No definite difference was found between the results of radon treatment and contact roentgen therapy, but in view of the difficulty in controlling the dosage when using radon, and the hazards involved, the latter treatment is to be preferred.

ZUSAMMENFASSUNG

Das Material besteht aus 20 Augen (11 Fälle) mit Conjunctivitis vernalis, welche mit Radon und Röntgenkontakttherapie behandelt worden sind. Sie sind danach 2—11 Jahre lang gefolgt worden. Achtzehn sind völlig geheilt und 2 bedeutend verbessert worden. Die beiden Therapieformen werden besprochen. Kein definitiver Unterschied konnte zwischen den Resultaten der Radonbehandlung und der Röntgenkontakttherapie festgestellt werden. Im Hinblick auf die Schwierigkeiten mit der Kontrolle der genauen Strahlendosis bei Benutzung von Radon sowie auf das mit dieser Methode verbundene Strahlenrisiko ist jedoch die Röntgenkontakttherapie vorzuziehen.

RÉSUMÉ

Les auteurs ont étudié 20 yeux (11 cas) atteints de conjonctivite printanière traités par le radon et par la roentgenthérapie de contact, et suivis pendant 2 à 11 ans. Dix-huit ont guéri complètement et 2 ont été considerablement améliorés. Les auteurs examinent ces deux formes de traitement. Ils n'ont pas trouvé de différence nette entre les résultats du traitement par le radon et ceux de la roentgenthérapie de contact, mais, étant donné qu'il est difficile de déterminer la dose quand on utilise le radon et que celà comporte des dangers, il faut préférer la roentgenthérapie de contact.

REFERENCES

BURNAM, C. F. and NEILL, JR., W.: Use of beta ray of radium applicator. Description of method and results obtained in superficial lesions of the eye. South. med. J. 33 (1940), 279.

CEDERLUND, J., LIDÉN, K. and LINDGREN, M.: Radiation hazards during radon treatment of eye lesions. Acta radiol. 48 (1957), 205.

FRICKE, R. E.: Beta irradiation of nonmalignant eye conditions. Ann. West. Med. Surg. 5 (1951), 125.

FRIEDELL, H. L., THOMAS, C. I. and KROHMER, J. S.: A Sr^{90} surface applicator designed for treatment of corneal lesions and evaluation of biological effects. Proc. Intern. Conf. Geneva, August 1955. Vol. 10. Radioactive isotopes and nuclear radiations in medicine. United Nations, New York 1956.

HAGUE, E. B.: Effective and safe radiation of the anterior segment of the eye. Amer. J. Ophthal. 35 (1952), 629.

ILIFF, CH. E.: Beta ray radium applicator for ocular use. Preliminary report. Arch. Ophthal. 38 (1947), 827.

— Present status of beta irradiation in ophthalmology. Concil. ophthal. XVI, London 1950. Acta Vol. 2 (1951), 1357.

LARSSON, S.: Notes on ophthalmological practice in Lund. Brit. J. Ophthal. 37 (1953), 257.

LEDERMAN, M.: Radiotherapy in the treatment of non-malignant superficial eye lesions. Proc. Roy. Soc. Med. 40 (1947), 573.

— Radiotherapy of disease of the cornea. J. Pac. Radiol. 4 (1952), 97.

— Some applications of radioactive isotopes in ophthalmology. Brit. J. Radiol. 29 (1956), 1.

MACDONALD, J. E., HUGHES, W. F. and PEIFFER, V. G.: Beta radiation cataracts. Arch. Ophthal. 53 (1955), 248.

MERRIAM, JR., G. R.: Late effects of beta radiation on the eye. Arch. Ophthal. 53 (1955), 708.

— The effects of beta radiation on the eye. Radiology 66 (1956), 240.

PENDERGRASS, E. P. and ANDREWS, J. R.: The radium emanation treatment of vernal catarrh. Am. J. Roentgenol. 34 (1935), 637.

VON SALLMAN, L., MUNOZ, C. M. and DZUNGIS, A.: Effects of beta irradiation on the rabbit lens. Arch. Ophthal. 50 (1953), 727.

SINCLAIR, W. K. and TROTT, N. G.: The construction and measurement of beta-ray applicators for use in ophthalmology. Brit. J. Radiol. 29 (1956), 15.

FROM THE DEPARTMENT OF RADIOTHERAPY (DIRECTOR: B. EBENIUS) AND THE RADIATION PHYSICS DEPARTMENT (DIRECTOR: K. LIDÉN), UNIVERSITY OF LUND, SWEDEN

RADIATION HAZARDS DURING RADON TREATMENT OF EYE LESIONS

by

J. Cederlund, K. Lidén, and *M. Lindgren*

Treatment of eye lesions with beta radiation from a radon applicator was introduced in Lund in 1949 by EBENIUS et coll. (CEDERQUIST, CRISTIANSSON, EBENIUS, and LARSSON 1957), who used essentially the same method as that described by ILIFF 1947, in which the radon glass bulb was enclosed in a metal container attached to a 36 cm rod. The radiologist was protected against the beta radiation from the applicator by lead rubber gloves and apron, but no special precautions were taken against the gamma radiation. After the introduction of a film badge control in 1951 for all the personnel in the department it was found that those radiologists carrying out this type of treatment were receiving a considerable amount of radiation. The hazards were therefore made the object of a detailed investigation.

The radiologist stands at the end of the table behind the head of the patient during the treatment and places the applicator on the point to be treated, remaining in this position in order to watch the patient continuously as the treatment is carried out. The treatment time is about 2 minutes for a 50 mC source, which is the one usually employed at this department.

Submitted for publication 4 May 1957.

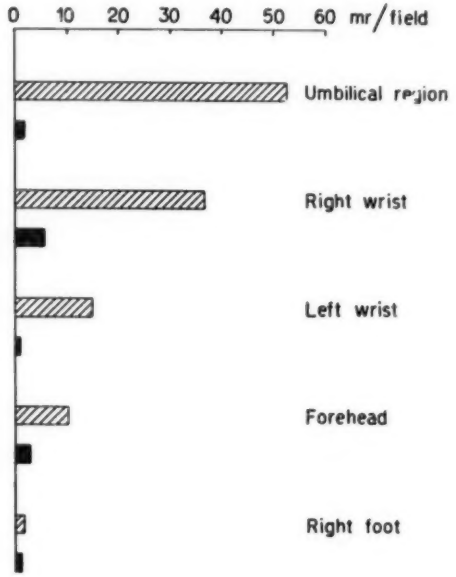

Diagram 1. Dose measured at different parts of radiologist during a two minute eye treatment with a 50 mC radon applicator. Hatched columns denote the mean doses measured before introduction of protection device (fig. 1) and black columns the mean doses measured after it was in position.

The doses received by the radiologist to five different parts of the body during the course of ten such treatments were determined. The measurements were made with ionization chambers of the English type BD 11, which were used at the department in earlier investigations of radiation hazards (LIDÉN & LINDGREN 1952). Pairs of such chambers were placed on the forehead, over the umbilical region, on the right foot, and on the right and left wrist of the radiologist. The measurements noted are summarized in Diagram 1 (hatched columns).

Every other week one and the same radiologist carried out 10 to 15 treatments, which implies that during this work alone he was exposed to more than the maximum permissible body dose of 300 mr per week. The doses measured were found to be greatest in the abdominal region, which in the evaluation of the total permissible dose is the most important. A protection shield of iron blocks was consequently designed so as to enclose the patient's head in order to decrease the undesirable leakage of radiation (Fig. 1). The shield is 10 cm thick between the patient and the radiologist and 5 cm thick on either side of and beneath the head of the patient; a lead container holds the applicator when it is not in use.

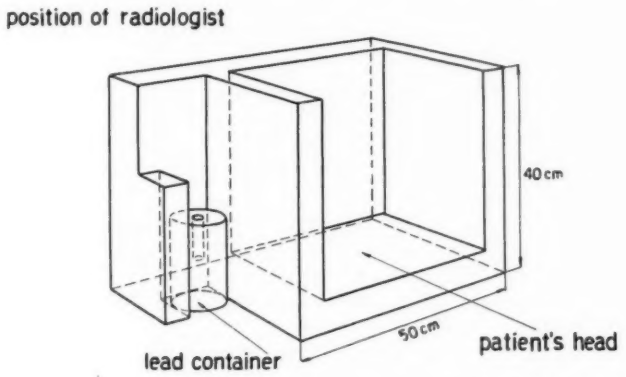

Fig. 1. Protection device consisting of iron blocks around head of patient during the treatment. The barrier is 10 cm thick between the patient and radiologist, and 5 cm on either side of and beneath the head of the former.

This arrangement has three advantages:

1. The walls absorb a large proportion of the radiation.
2. The radiologist is exposed to radiation only during the actual treatment.
3. The distance between the patient and the radiologist is automatically increased.

The radiation received by the radiologist since the introduction of this arrangement was studied in the same way as before. The results are given in Diagram 1 (black columns). It is evident that the device decreases the hazards of radiation considerably. The total dose received by the radiologist is now only about one tenth of the maximum permissible dose per week. The investigation thus shows that it is possible with simple measures to provide reasonable protection even in a case where the radiologist has to handle a gamma ray source of about 50 mC for some minutes.

As to the assistants, no significant change was found between the dose received before and after the introduction of the protection arrangement. The dose they received was barely measurable, about 2 to 3 mr per treatment and thus negligible.

SUMMARY

The radiation hazards of beta-ray treatment of eye lesions with a radon applicator were studied. A protective barrier producing a 90 per cent reduction in the gamma radiation recived by the radiologist is described.

ZUSAMMENFASSUNG

Das Strahlenrisiko bei der Betastrahlenbehandlung von Augenkrankheiten mit einem Radonapplikator ist untersucht worden. Ein Schutzwall wurde konstruiert, welcher die den Radiotherapeuten treffende Gammastrahlung mit 90 % reduzierte.

RÉSUMÉ

Les auteurs étudient les risques de radio-lésions dans le traitement par le rayonnement bêta de lésions oculaires par un applicateur de radon. Ils étudient un dispositif de protection qui réduit de 90 % la dose gamma reçue par le radiologiste.

REFERENCES

Ebenius, B., Larsson, S., Cederquist, E. and Cristiansson, J.: Radiation therapy of vernal conjunctivitis. Acta radiol. 48 (1957), 193.

Iliff, C. E.: Beta irradiation in ophthalmology. Arch. Ophthal. 38 (1947), 415.

Lidén, K. and Lindgren, M.: Radiation hazards during cholangiographic examinations. Acta radiol. 38 (1952), 1.

FROM THE ONTARIO CANCER FOUNDATION, LONDON CLINIC (DIRECTOR: IVAN H. SMITH), VICTORIA HOSPITAL, LONDON, ONTARIO, CANADA

IDEALIZED BODY CONTOURS IN ROTATION DOSIMETRY

by

Robert H. Haynes and *Gerd Froese*

From both a physical and a clinical viewpoint, the determination of the complete isodose distribution in all forms of radiotherapy is the ideal approach to the problem of clinical dosimetry. However, in the case of 360° rotation therapy, the use of the central tumour dose as a practical clinical measure is well recognized, and so the authors have developed a rapid method for calculating this dose which requires only the measurement of the anteroposterior and lateral dimensions of the patient. This method specifically enables one to calculate the *water-equivalent 'tumour-air ratio'* for 360° rotation. The clinical data presented in this paper were obtained from patients treated with the Cobalt 60 teletherapy units built by Atomic Energy of Canada Limited, at a source-tumour distance of 75 cm with the AECL Model B theratron, and at 95 cm with the Model A unit and auxiliary rotation equipment as described by PFALZNER and INCH (1956). Although we shall consider only 360° rotation with Cobalt 60 teletherapy, the method can be extended to roentgen ray rotation therapy and also to sector rotation.

General description of idealized contour method. JOHNS, WHITMORE, WATSON and UMBERG (1953) made use of the tumour-air ratio (denoted by $R(r)$) based on depth dose data obtained in water as a means of calculating central axis tumour dose in rotation therapy. This method, which we shall hereafter refer to as 'Johns' meth-

Submitted for publication 21 February 1957.

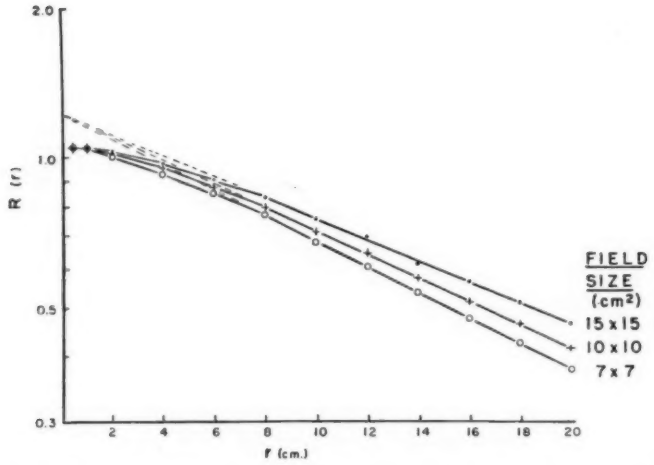

Diagram 1. The tumour-air ratio, $R(r)$, plotted semi-logarithmically, for three field sizes.

od', consists in averaging the tumour-air ratios defined by the tumour skin radii every 10° or 20° around the patient's contour; the actual tumour dose is then determined by multiplying the 'averaged tumour-air ratio' $\bar{R}$ by the air dose at the tumour in accordance with the definition of $R(r)$. This gives sufficiently accurate results for most clinical purposes, within the limits of the water equivalence assumption, and can be applied with equal ease to both central and eccentric tumours. However, in practice the method is somewhat laborious and time-consuming, which is a disadvantage in clinics with a large patient volume. The idealized contour method is a mathematical extension of Johns' method, in that we have found a simple two-parameter family of curves, the members of which can be fitted very accurately to the particular body contours encountered clinically in rotation therapy. Therefore it is possible to fit an appropriate idealized contour to any given contour and integrate the tumour-air ratio function, $R(r)$, about the idealized contour to obtain the 'average tumour air ratio', $\bar{R}$ for 360° rotation. The average tumour-air ratio obtained in this way is a function of the anteroposterior and lateral dimensions of the patient. We have evaluated this function over the range of dimensions encountered clinically, so that having measured the above distances either directly by calipers or from a contour diagram, the average tumour-air ratio can be obtained immediately from the tables or graph of this function.

Empirical representation of $R(r)$. The tumour-air ratio $R(r)$ as defined by NEUMANN and WACHSMANN (1942) and JOHNS et coll. (1953)

Table

Empirical constants in $R(r)$ for Co^{60}

Field size	A_1	a_1	A_2	a_2
5×5 cm^2	1.210	0.0645	− 0.178	0.364
10×10 cm^2	1.269	0.0562	− 0.243	0.393
15×15 cm^2	1.221	0.0473	− 0.210	0.460

is the ratio of the radiation dose in a water phantom at a given distance from the source (source-tumour distance S.T.D.) to the dose in air at the same point in space, and is usually plotted as a function of the thickness of water between this point and the source. It is clear, therefore, that $R(r)$ can be calculated from the central-axis depth dose and backscatter data of a given source and at any given tumour distance from that source. We have calculated $R(r)$ from the depth dose data of JOHNS (1953) for Cobalt 60 radiation at 75 cm S.T.D. This data is plotted logarithmically in Diagram 1 and can be closely represented over the range $2 \leq r \leq 20$ cm by the double exponential

$$R(r) = A_1\, e^{-a_1 r} + A_2\, e^{-a_2 r} \quad \ldots\ldots\ldots\ldots\ldots\ldots (1)$$

This range of r is more than adequate to cover all rotation cases encountered clinically. The constants in equation (1) for three field sizes are given in the Table above. We have not attached any physical significance to these constants and for our purpose they are simply the best empirical fit over the range indicated in this representation of $R(r)$.

The idealized body contours. When examining typical body contours (cross-sections) one would naturally think of the ellipse as being a good representation of their general shape. Therefore we attempted to integrate the tumour-air ratio function about an ellipse. The resulting integrals cannot be evaluated in terms of elementary functions, and although it is possible to avoid these integrals by suitable approximations, and thereby develop a method that gives reasonably good results in practice, the use of the ellipse as an idealized contour was abandoned when a more suitable contour was developed.

The equation of the ellipse with semi-major axis a and semi-minor axis b is, in polar form,

$$r^2 = \frac{a^2 b^2}{a^2 \sin^2\theta + b^2 \cos^2\theta} \quad \ldots\ldots\ldots\ldots\ldots\ldots (2)$$

or alternatively,

$$r^2 = \frac{a^2}{1 + (k^2 - 1)\sin^2\theta} \quad \ldots\ldots\ldots\ldots\ldots\ldots (3)$$

where $k = \dfrac{a}{b}$ is the axial ratio.

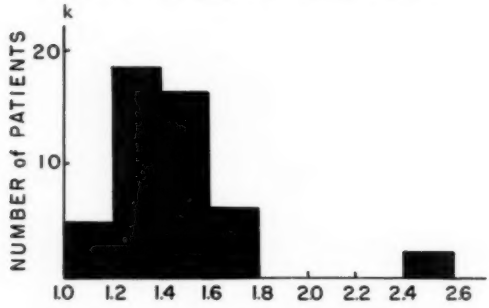

Diagram 2. Distribution of axial ratios (k) in a clinical series of 48 rotation cases.

Expanding (3) in powers of $\cos 2\theta$ we get,

$$r = \sqrt{\frac{2a^2}{1+k^2}}\left[1 - \frac{K}{2}\cos 2\theta + \frac{3}{8}K^2\cos^2 2\theta - \ldots\right] \quad \ldots\ldots (4)$$

where $K = \dfrac{1-k^2}{1+k^2}$. Consider the first two terms of (4) which are of the form,

$$r = A - B\cos 2\theta, \quad A \geq B;\ A > 0,\ B \geq 0 \quad \ldots\ldots (5)$$

This function is 'oval' in appearance, is symmetric with respect to the origin, and is readily integrable in closed form. Thus it is clearly a suitable approximation to body contours. Since the semi-major and semi-minor axes (a, b) of the patient are the most easily measured dimensions, we must find the simplest transformation of A and B in terms of a and b, in order to fit (5) to actual body contours. The expansion coefficients in (4) are not very simple functions of a and b, which is due primarily to the fact that the long axis of the curve represented explicitly by the first two terms of (4) is rotated through 90° with respect to the major axis of the original ellipse. Thus the simplest procedure is to set the long axis of (5) equal to the patient's lateral dimension (major axis) and the short axis of (5) equal to the patient's anteroposterior dimension (minor axis), viz.,

$$\begin{aligned} r_{max} &= r(\pi/2) = A + B \equiv a \\ r_{min} &= r(0) = A - B \equiv b \end{aligned} \quad \ldots\ldots (6)$$

whence

$$\begin{aligned} A &= (a+b)/2 \\ B &= (a-b)/2 \end{aligned} \quad \ldots\ldots (7)$$

Thus in order to approximate a body contour by a function of the form (5) one simply has to set A and B equal to the semi-sum and semi-difference respectively of the patient's semi-major and semi-minor axes.

We must now examine the function (5) in somewhat more detail in

order to determine its limits of validity as an idealized body contour. The shape of (5) changes considerably with changes in the relative magnitudes of A and B. It is clear that for $B = 0$, the function represents a circle of radius A. As B increases from zero, the radii near $\theta = 0$ become shorter than the radii near $\theta = \pi/2$ so that the function becomes oval in shape. As B continues to increase toward the value of A, the 'constriction' of these radii becomes more pronounced until the 'oval' has degenerated into two lobes when $B = A$, *i. e.* $r(0) = r(\pi) = 0$ for $B = A$. If this constriction of the curve were to occur too rapidly with respect to changes in B, the function could not be used as an idealized body contour since it would not allow for sufficient elongation before changing to a constricted oval. Therefore it is essential that the curve be at most only slightly constricted for axial ratios very close to those most commonly occurring in the human torso. The remarkable result is that the curve is flat at $\theta = 0$ for $k = 1.5$, which is very close to the average axial ratio ($k = 1.47$) of the 48 body contours which we have encountered clinically. To show this, we begin by superimposing a rectangular coordinate system on the polar equation (5) so that the $\theta = 0$ radius coincides with the positive x-axis and the $\theta = \pi/2$ axis coincides with the positive y-axis. The semi-minor axis of the patient is equal to the maximum value of the x-component of the radius arm, denoted by $r_{x\ max}$, as long as the curve is not constricted at $\theta = 0$, according to the transformation (7). Therefore we must calculate the conditions on A and B, and thence on k, such that $r_{x\ max}$ occurs at $\theta = 0$, for when the function begins to constrict, $r_{x\ max}$ moves away from $\theta = 0$.

The maximum value of r_x occurs for values of θ such that,

$$\frac{d}{d\theta} r \cos \theta = 0 \quad \ldots\ldots\ldots\ldots\ldots\ldots \quad (8)$$

$$i.\ e.,\ [6\ B \cos^2 \theta - (A + B)] \sin \theta = 0$$

and is satisfied for $\sin \theta = 0$, or $\theta = 0, \pi$ as implied by (7), and for,

$$\cos^2 \theta = (A + B)/6\ B \ldots\ldots\ldots\ldots\ldots\ldots \quad (9)$$

after constriction has begun. It is clear that the condition on A and B such that the contour (5) is flat (*i. e.*, changing from convex to concave) at $\theta = 0$ is given by,

$$\frac{d^2}{d\theta^2} r \cos \theta \Big|_{\theta = 0} = 0 \quad \ldots\ldots\ldots\ldots\ldots\ldots \quad (10)$$

$$i.\ e.,\ -(A + B) + 6\ B = 0$$

whence,

$$A = 5\ B,\ \text{or}\ k = (A + B)/(A - B) = 3/2 \quad \ldots\ldots\ldots \quad (11)$$

Therefore the shape of (5) is circular for $B = 0$ or $k = 1$, and so convex near $\theta = 0$. As B or k increases this convexity diminishes and the curve

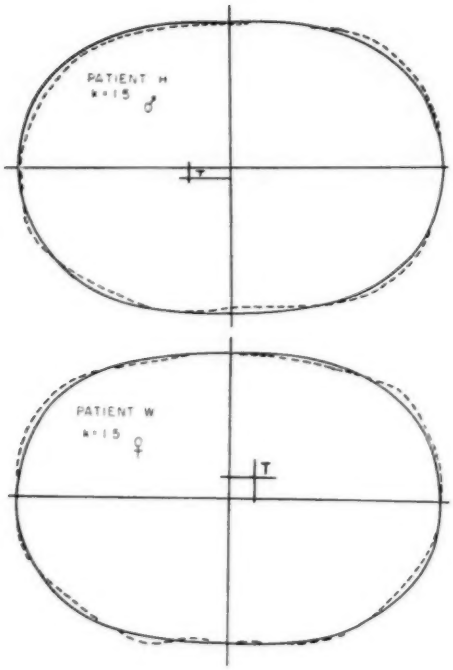

Diagram 3. Comparison of the idealized body contour with two actual thoracic contours in the series studied. The broken line is the patient's outline and the tumour centre is indicated by its coordinates with respect to the centre of the contour.

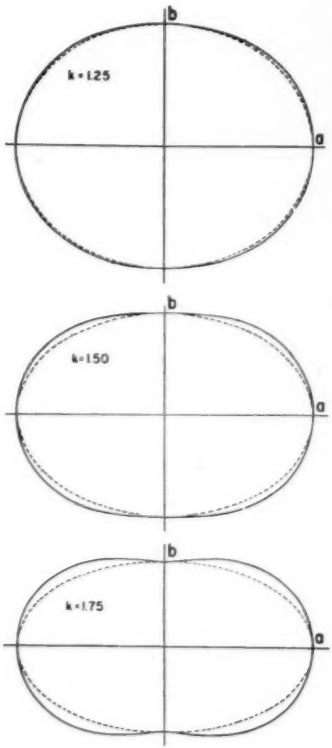

Diagram 4. Comparison of the idealized body contour (equation (5)) with the ellipse (broken line) for three axial ratios.

is flat at $\theta = 0,\pi$ for $B = 1/5$ or $k = 1.5$. For values of $k > 1.5$ the curve constricts or is concave at $\theta = 0,\pi$. The transformation equations (7) therefore apply for $1 \leq k \leq 1.5$, if one wishes to impose the condition that $r_{x\ max} = b$.

For axial ratios greater than 1.5, $r_{x\ max}$ does not occur at $\theta = 0$ so that $r_{x\ max} = b$. However, the transformation (7) can still be used, since the constriction is not very rapid, and for $k = 1.75$, $r_{x\ max}$ is only 3 % greater than $r(0)$. In this range it need only be remembered that $r_{x\ max}$ is slightly greater than b, and occurs for θ as given by equation (9).

The distribution of k among 48 body contours is indicated in Diagram 2. The authors feel that this idealized contour should not be used for axial ratios greater than 1.8 due to the constriction effect, and so $\bar{R}$ has been evaluated on the range $1.0 \leq k \leq 1.8$. As indicated above, it is indeed most fortunate that the typical axial ratio should be 1.5, so that equation (5) is particularly applicable to body contours since they are usually somewhat flattened on the anterior and posterior surfaces. Two typical contours from the thoracic region of a male and female are compared in Diagram 3 with the idealized contour fit according to the transformation (7).

The idealized body contour (5) is compared in Diagram 4 with the ellipse for three axial ratios in the range encountered clinically. It is also clear from this comparison that (5) is a better representation of the human torso than the ellipse at the higher axial ratios because it is not so truncated with respect to the major axis.

Calculation of $\bar{R}$: tumour at centre of contour

Having found a simple empirical representation for $R(r)$ and a suitable idealized body contour (5), it is now a simple matter to calculate the average value of $R(r)$ for 360° rotation about centrally located tumours.

We have immediately,

$$\bar{R} = \frac{2}{\pi} \int_0^{\pi/2} [A_1 e^{-a_1 r(\theta)} + A_2 e^{-a_2 r(\theta)}] \, d\theta \quad \ldots\ldots\ldots\ldots\ldots\ldots\ldots\ldots \quad (12)$$

where $r(\theta) = A - B \cos 2\theta$, and the integration need be extended over one quadrant only due to the symmetry of the contour.

The form of $r(\theta)$ enables us to take the major contribution to $\bar{R}$ outside the integral as a constant factor so that approximations in the integral itself will involve only a small part of $\bar{R}$, viz.,

$$\bar{R} = \frac{2}{\pi} A_1 e^{-a_1 A} \int_0^{\pi/2} e^{a_1 B \cos 2\theta} \, d\theta + \frac{2}{\pi} A_2 e^{-a_2 A} \int_0^{\pi/2} e^{a_2 B \cos 2\theta} \, d\theta \ldots\ldots \quad (13)$$

Expanding the exponentials and integrating, the odd powered terms vanish and the series converges rapidly so that one can neglect the even terms of the 4th order and higher. The neglect of the 4th order term introduces an error of only one part in one thousand. Thus only the zeroth and 2nd order terms remain and we have,

$$\bar{R}\ (A, B) = A_1 e^{-a_1 A}[1 + \tfrac{1}{4} a_1^2 B^2] + A_2 e^{-a_2 A} [1 + \tfrac{1}{4} a_2^2 B^2] \ldots\ldots \quad (14)$$

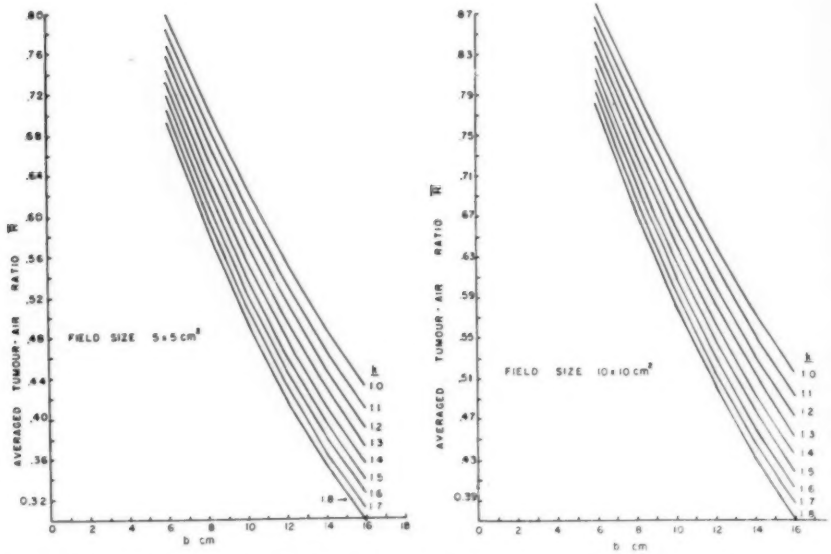

Diagrams 5 and 6. Curves of $\overline{R}(b,k)$ used in the clinical series studied; calculated from equation (15) and the constants in the table.

Using (7) and writing in terms of the parameters b and k we get finally,

$$\overline{R}(b,k) = A_1 e^{-\frac{1}{2}a_1 b(k+)1}[1 + \tfrac{1}{16} a_1^2 b^2 (k-1)^2] + \\ + A_2 e^{-\frac{1}{2}a_1 b(k+1)}[1 + \tfrac{1}{16} a_2^2 b^2 (k-1)^2] \quad \ldots\ldots\ldots\ldots \quad (15)$$

The fact that $\overline{R}$ is written as a function of the parameters b and k can be indicated by the notation $\overline{R}(b,k)$. Since a and b are the parameters that are measured directly it may appear that the choice of b and k in (15) is not the simplest from the point of view of routine calculation. However, since the axial ratio k is a useful parameter for the characterization of the body contour, and since the degree of constriction of the idealized contour is most conveniently expressed in terms of the magnitude of k, the authors decided to use these parameters rather than (a, b).

We have evaluated (15) over the range of b encountered clinically and for $1.0 \leq k \leq 1.8$. It is clear from the histogram of k that this range encompasses virtually all values of k that are apt to occur. $\overline{R}(b, k)$ is shown in Diagrams 5, 6, 7, as a function of b for the field sizes 5×5 cm², 10×10 cm² and 15×15 cm² respectively, and for a S.T.D. of 75 cm. The tumour-air ratios used as the basis for these calculations were based

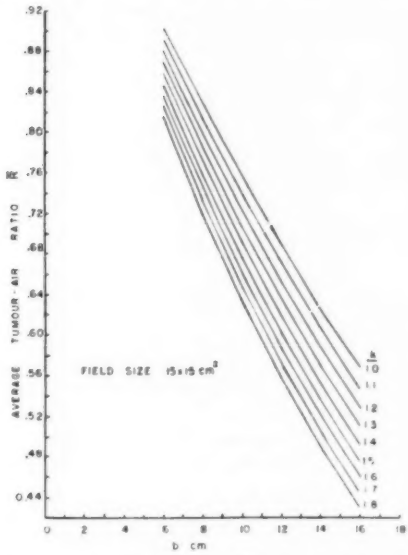

Diagram 7. Curves of $\overline{R}(b, k)$ used in the clinical series studied; calculated from equation (15) and the constants in the table.

on the older depth dose data of JOHNS (1953) so that there was a slight dependence on the source-tumour distance. At present we are recalculating $\overline{R}(b, k)$ on the basis of the latest tumour-air ratio values of JOHNS, MORRISON and WHITMORE (1956) which are valid for all source-tumour distances in the range 40—100 cm, and which are themselves based on more recent backscatter values. These revised values will be published as soon as they are available.

Calculation of $\overline{R}$: non-central tumour

The calculation of $\overline{R}$ for a non-central tumour involves writing the equation of the contour in the form,

$$\varrho = f(\varphi) \quad \ldots\ldots\ldots\ldots\ldots\ldots\ldots\ldots \quad (16)$$

where (ϱ, φ) are the polar coordinates of the contour in the coordinate system obtained by translating the origin from the geometrical origin of the contour to the position of the tumour. It is then possible, in principle, to average R about the contour with respect to the new origin, *i. e.*,

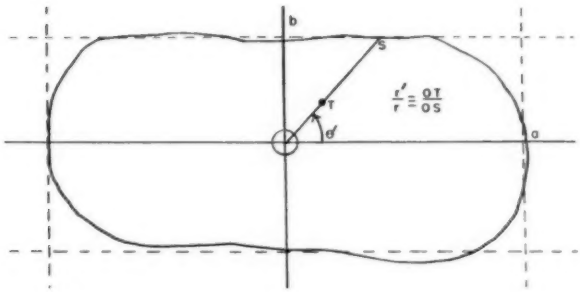

Diagram 8. Diagram illustrating method of 'boxing in' contour (not an actual patient) to obtain contour parameters a, b and r'/r. The tumour centre is at T and the polar coordinates of T with respect to the contour centre are (r', θ'). The tangents to the anterior and posterior surfaces are usually the most difficult to locate due to the necessity of 'balancing', area-wise, the contour irregularities.

$$\bar{R}' = \frac{1}{2\pi} \int_0^{2\pi} R\ (\varrho)\ d\varphi \quad \ldots\ldots\ldots\ldots\ldots\ldots\ (17)$$

Now although it is easy to translate axes and write (16) as an implicit function of the form,

$$F\ (\varrho, \varphi) = 0 \quad \ldots\ldots\ldots\ldots\ldots\ldots\ (18)$$

it is difficult to write (18) in the explicit form required for (17), and the attendant mathematical complications make the evaluation of (17) virtually impossible. Because of these mathematical difficulties, and since the difference between (17) and (12) is small for tumours which are sufficiently central to make rotation the treatment of choice, the authors decided that the best approach to the problem of the non-central tumour would be to actually calculate by Johns' method the averaged tumour-air ratio within the idealized contour and compare this with the averaged tumour-air ratio at the centre of the contour, as obtained from (12) and (15).

Thus let $\bar{R}'_j$ be the averaged tumour-air ratio for 360° rotation calculated by Johns' method at the tumour, (r', θ'), and $\bar{R}$ be, as usual, the averaged tumour-air ratio for 360° rotation about the centre of the contour, as given by (15). We can therefore define the 'eccentric correction factor' C_e by the ratio,

$$C_e = \bar{R}'_j / \bar{R} \quad \ldots\ldots\ldots\ldots\ldots\ldots\ (19)$$

We risk, perhaps, some confusion in calling C_e the eccentric correction factor. It must be remembered that the word 'eccentric' in this context

refers to the fact that the tumour is located off-centre or 'eccentrically', and not to the 'eccentricity' of the contour which is described by the axial ratio k. Now we must find a suitable measure for the degree of eccentricity (of 'off-centeredness') of any given tumour and then investigate the behaviour of C_e in terms of the possible range of variation of such parameters as field size, size and shape of the contour and the position of the tumour within the contour. Having thus calculated C_e, we can correct $\bar{R}$ for eccentricity, viz.,

$$\bar{R}' = C_e \bar{R} \quad \ldots\ldots\ldots\ldots\ldots\ldots\ldots\ldots \quad (20)$$

where $\bar{R}'$ is the 'idealized contour value' at (r', θ').

The eccentric correction factor C_e

The ratio of the distance between contour centre and tumour to the radius vector of the contour which passes through the tumour, r'/r, has been found to be a simple and rational measure of the eccentricity of the tumour. And, as is shown below (Diagram 11) the differences between $\bar{R}$ and $\bar{R}'$, in a series of 48 cases is well correlated with this measure of eccentricity.

The parameters which affect C_e are discussed below and a set of C_e curves for different values of these parameters is shown in Diagram 8. We have found that the variation in these parameters that occurs clinically can be sub-divided and grouped so that the curves in Diagram 8 are all that need be used. In fact, as will also be shown from statistical considerations, this set of C_e curves can be replaced in practice by a single curve, which is averaged with respect to the indicated parameters, without significantly affecting the results.

a) *Angular orientation of r'.* The maximum possible variation of $C_e(r'/r)$ with θ was determined by calculating $C_e(r'/r)$ for tumours lying along the positive y-axis and positive x-axis of a typical contour ($k = 1.5$, $b = 11$). In this way it was found that the effect of θ on C_e is completely negligible over the practical range of r'/r and that the slight reduction ($\approx 1\ \%$) in C_e that does occur along the y-axis is for values of $r'/r > 0.6$ which is of no clinical interest from the point of view of rotation therapy. Accordingly, for the rest of the calculations the tumour was located on the positive x-axis and $C_e(r'/r)$ considered to be independent of θ.

b) *Shape factor of contour.* There is a slight dependence of $C_e(r'/r)$ on k, but once again this is negligible except for $r'/r > 0.6$. For $r'/r = 0.6$, and the typical contour used above, the difference between C_e for k's of 1.25 and 1.75 is less than 2 %, and this decreases rapidly for $r'/r < 0.6$. Therefore all further calculations were made for contours in which $k = 1.50$, which is not only an average with respect to the variation in

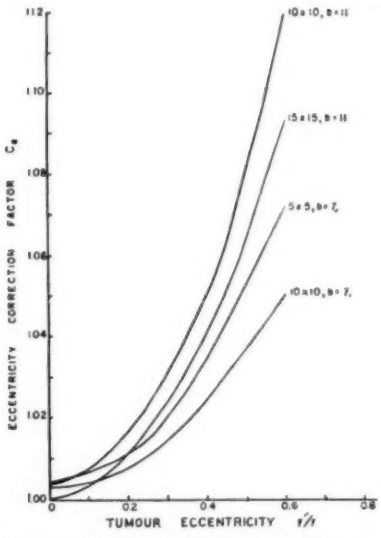

Diagram 9. Eccentricity correction factor, $C_e(r'/r)$, used to correct $\overline{R}$ with the parameter grouping scheme indicated in the text. All of these curves were obtained from contours for which $k = 1.50$.

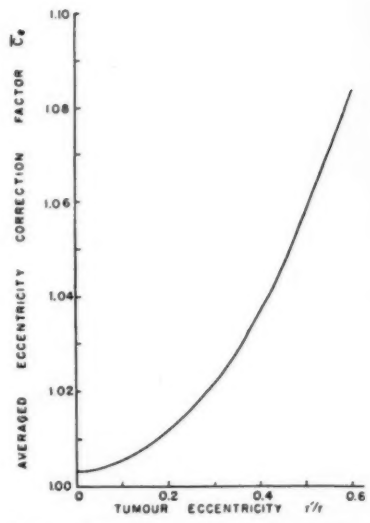

Diagram 10. Averaged eccentricity correction factor $\overline{C}_e(r'/r)$ obtained by averaging the ordinates of the curves of diagram 9.

C_e caused by k but is also the average shape factor of the contours that occur clinically. Thus the net effect on C_e of assuming this constant value for k is completely negligible except for the most eccentric tumours that would possibly be rotated, and even in these few cases is less than 1 %.

c) *Absolute size of contour and field size.* We have now effectively eliminated two of the four parameters that might be expected to affect C_e: θ has a negligible effect on C_e in the clinical range and so need not be considered at all and the effect of k can be neglected if a suitably chosen average value is used throughout the calculations. The remaining parameters, field size and the semi-minor axis of the contour (which determines the absolute size of the contour for a given k) have a significant effect on C_e for $r'/r > 0.25$, and which becomes more marked as r'/r increases. From the curves of Diagram 9 it is clear that b and field size have reciprocal effects on the value of C_e; and since larger field sizes tend to be used with larger contours, and certainly smaller field sizes with smaller contours, these parameters tend to compensate, so that the range of C_e used in practice is not too great. In fact, it is possible to use

a single correction curve for all values of the above mentioned parameters without significantly changing the difference between $\overline{R}'$ and $\overline{R}'_j$.

From the clinical standpoint, the range of b in 48 cases was found to lie within 5 and 14 centimeters and the distribution tended to be bimodal; that is to say, the cases could be divided roughly into two groups, a smaller group of head and neck cases with a mean value close to 7 cm, and a larger group of thoracic and abdominal cases with a mean value close to 11 cm. We therefore used these two values to group the cases with respect to the parameter b: cases in the range $5 \leq b < 9$ were corrected, using the C_e curves corresponding to $b = 7$ for the two field sizes used (5×5 cm, 10×10 cm) and cases in the range $9 \leq b \leq 14$ were corrected using the C_e curves corresponding to $b = 11$, for the three field sizes used (5×5 cm, 10×10 cm, and 15×15 cm).

In this series only square fields were used of the dimensions indicated. In the case of rectangular fields of intermediate area, one would use the curve for the field area which was closest to the one actually used. The error introduced by this approximation is clearly insignificant.

Average eccentric correction curve. The average eccentric correction curve, shown in Diagram 10 represents a mean of the family of curves in Diagram 9. We shall denote the values of C_e obtained from this curve by $\overline{C}_e$. Inasmuch as little or no physical advantage is gained by rotating tumours which are more eccentric than $r'/r = 0.4$, and considering the small size of C_e on the range $0 \leq r'/r \leq 0.4$, it is clear that the use of the average eccentric correction curve is well justified in practice. Our clinical series of 48 cases has been corrected using both the curves of Diagram 9 and the average curve of Diagram 10 and the statistical analysis of the results, as described below, indicate no significant difference between the two methods of correction.

Clinical comparison of Johns' method with the idealized contour method

The idealized contour method and Johns' method (measuring radii at 20° intervals) were applied to a series of 48 cases, 39 of which were treated with the AECL Model B theratron at the Windsor Clinic of the Ontario Cancer Foundation and the remaining 9 treated with the AECL Model A Cobalt 60 teletherapy unit and auxiliary rotating equipment at the London Clinic of the Ontario Cancer Foundation. The composition of this series of cases was as follows: of the total of 48 cases, 36 were carcinomas located in the thoracic and abdominal regions and 12 were located in the head and neck. Of the thoracic and abdominal sites, 16 were bronchogenic, 6 oesophageal, 5 gastric, 3 lower intestinal and 6 in miscellaneous sites. In all of these cases, body cross-sections in the treatment plane were

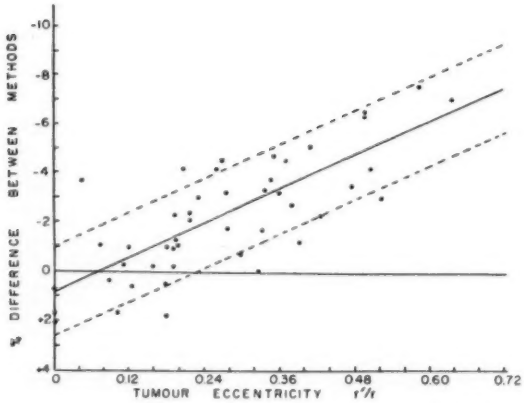

Diagram 11. Scatter diagram of the percentage differences between $\overline{R}$ and $\overline{R}'_j$. The negative percentages indicate that $\overline{R}$ is less than $\overline{R}'_j$. The solid line is the regression of percentage difference on tumour eccentricity and the broken lines correspond to one standard error of estimate. The correlation coefficient is 0.66.

obtained, using heavy lead solder wire in the usual way. The parameters a and b were determined from the cross-section diagrams by 'boxing in': that is, parallel tangents were drawn to the anterior and posterior surfaces and similarly to the lateral surfaces, the lateral tangents being drawn perpendicular to the anterior-posterior tangents (Diagram 8). The distances between these tangents are 2b and 2a respectively from which (b, k) was obtained. Having obtained (b, k) in this way, $\overline{R}$ was read directly from the appropriate graph (Diagrams 5, 6, 7).

The differences between $\overline{R}$ and $\overline{R}'_j$ for these cases were calculated as a percentage of $\overline{R}'_j$, and plotted as a function of r'/r (Diagram 11). The equation of the regression line calculated by the least squares method is,

$$100\ (\overline{R} - \overline{R}'_j)/\overline{R}'_j = 0.8 \pm 0.5 - (11.6 \pm 1.7)\, r'/r \quad \ldots\ldots\ (21)$$

where the $\pm$ signs indicate the standard errors of the regression coefficients. The standard error of estimate, $S_y = \pm 1.84$ %, and is indicated in Diagram 11 by the dotted lines. The correlation coefficient is 0.66 ± 0.06, which gives a t ratio of 6.23 so that the correlation is highly significant ($p < 0.01$). The correlation was not significantly improved by using $(r'/r)^2$ as the independent variable.

This analysis of the differences between $\overline{R}$ and $\overline{R}'_j$ proves that we are justified in our assumption that this difference can be largely attributed to the fact that the tumour is off center and that the ratio r'/r is a valid measure of this 'off centeredness' or 'eccentricity'. Furthermore, the residual scatter that remains after that due to eccentricity has been removed is of the same order of magnitude as would be expected from the random error in the calculation of $\overline{R}'_j$ and $\overline{R}$ (approximately 2 %).

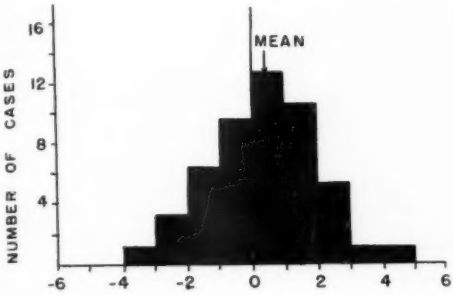

Diagram 12. Histogram of the percentage differences between $\overline{R}'$ and $\overline{R}'_j$ following correction of $\overline{R}$ by C_e (cf. diagram 9). The mean is + 0.38 % and the standard deviation is 1.73 %.

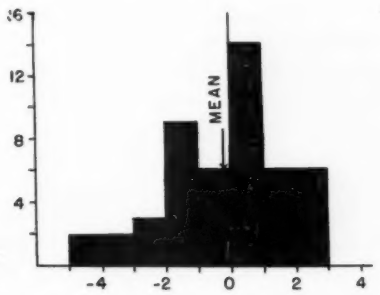

Diagram 13. Histogram of the percentage differences between $\overline{R}'$ and $\overline{R}'_j$ following correction of $\overline{R}$ by $\overline{C}_e$ (cf. diagram 10). The mean is — 0.14 % and the standard deviation is 1.80 %.

The values of $\overline{R}$ were corrected for eccentricity as indicated in (20) using both the C_e curves given in Diagram 9 and the averaged correction, $\overline{C}_e$ given in Diagram 10. Thus we obtained two sets of averaged tumour-air ratio values corrected for eccentricity and in both cases we use the notation $\overline{R}'$ to denote the corrected value. The statistical effect of these methods of correction can be better appreciated by first considering the uncorrected distribution of percentage differences, that is, the distribution of the left hand side of (21): the mean uncorrected percentage difference with its standard error is -2.4 ± 0.1 %, the standard deviation is 2.46 %, and the mean is significantly different from zero ($t = 6.8$, $p \ll 0.01$). As we have seen, this difference from zero is correlated with eccentricity to a high degree of significance. The distribution of the percentage differences between $\overline{R}' = C_e\overline{R}$ (C_e from Diagram 9) and $\overline{R}'_j$ is shown in Diagram 12. The mean and standard error of this latter distribution is $+ 0.38 \pm 0.25$ and the standard deviation is 1.73 %; this gives a t ratio of 1.54 ($p > 0.1$) indicating no significant difference between $\overline{R}'$ and $\overline{R}'_j$. It should also be noted that the standard deviation has been reduced from 2.46 % to 1.73 %, a significant reduction (the standard deviations of the standard deviations are 0.25 % and 0.18 % respectively).

The distribution of percentage differences between $\overline{R}' = \overline{C}_e\overline{R}$ and $\overline{R}'_j$ is shown in Diagram 13. The mean and standard error of this distribution is -0.14 ± 0.26 and the standard deviation is 1.80 %; this gives a t ratio of 0.55 ($p > 0.5$) indicating no significant difference from zero as before. Thus there again is no statistically significant difference between $\overline{R}'$ and $\overline{R}'_j$ even when the averaged eccentricity correction factor,

C_e, is used to correct $\overline{R}$. Furthermore, the character of the distribution itself is not changed between the two methods of correction, insofar as there is no significant difference between the standard deviations of the two distributions; however, in the second case the mean is shifted slightly and the histogram is more irregular. One could, of course, use the regression line (21) as an eccentric correction factor; and although the rationale of such a procedure is not as satisfying as that of using $\overline{C}_e$, it is nevertheless of interest that the mean, standard deviation and t ratio of the resulting distribution of percentage differences are almost identical with those of the distribution in Diagram 13. This is not surprising since if the regression line (21) and $\overline{C}_e$ are superimposed it is clear that (21) is a good linear approximation to $\overline{C}_e$.

In summary then, the problem of the off-centered tumour can be handled by calculating the averaged tumour-air ratio for rotation about the centre of the contour, $\overline{R}$, and correcting this by means of an eccentric correction factor to get $\overline{R}'$. The use of C_e (Diagram 9) is perhaps more desirable from the academic standpoint, but in practice the use of $\overline{C}_e$ (or even the regression line (21)) is more sensible on account of its simplicity and the small size of the correction itself. Furthermore the correction exceeds the random error of the calculations only if the tumour is more eccentric than $r'/r = 0.35$.

Therefore in the vast majority of rotation cases the error introduced by neglecting the eccentric correction factor could be well tolerated from the clinical standpoint. A suggested rule-of-thumb is that C_e can be neglected for all those cases in which the tumour eccentricity r'/r is less than 0.3. However, whatever plan is adopted regarding the eccentricity correction, it should be adhered to in all cases for the sake of consistent statistics.

Discussion and Conclusions

We have developed a simple, rapid method for calculating the averaged tumour-air ratio in 360° rotation therapy which is essentially a mathematical extension of the well known method of Johns, and which gives results that do not differ significantly from those obtained by the latter, longer method. It suffers, of course, from the same malady that afflicts all other similar methods, namely, the use of water phantoms in the determination of $R(r)$. The error introduced by the assumption of a water equivalent absorber enclosed by the body contour has been discussed by many workers, and in this laboratory Inch and Haynes (1956) have found that the actual dose can be as much as 30 % higher in some

thoracic cases but averages about 20 %. If the treatment plane does not contain lung tissue the error is, of course, much less. Nevertheless in thoracic cases this is a serious error that must be taken into account clinically, but at the present time there are many clinics in which the facilities and personnel for making routine transit dose measurements are not available and so water equivalent methods must still be used. In such instances, the idealized contour method can greatly facilitate the estimation of tumour dose in rotation therapy. It is also useful, even when the transit dose is measured on each patient, as a simple preliminary estimation of the tumour dose, so that the treatment program can be planned and initiated, and the total dosage later adjusted when the transit dose measurements have been obtained.

Acknowledgements

From among the many people who helped to make this research possible the authors would like particularly to thank Dr. W. Rodger Inch of this clinic for suggesting the problem, for his work in the early days of this project, and for his continuing interest in it. Special thanks are also due to Mr. Arwell Evans of the Mathematics Department, University of Western Ontario, for helpful discussions and suggestions regarding the choice of idealized contour. We are greatly indebted to Dr. Ivan H. Smith and Dr. Norman A. McCormick, Directors of the London and Windsor Clinics respectively of the Ontario Cancer Foundation, for permission to use clinical data from their centers, and for their unfailing interest and encouragement during the course of this work. Finally, we would like to thank Professor Alan C. Burton of the Biophysics Department, University of Western Ontario, for many useful suggestions and guidance throughout the research.

We are indebted to the R. C. Mahon Foundation of Detroit, Michigan, U. S. A., for their generous financial support.

SUMMARY

The averaged tumour-air ratio in 360° rotation radiotherapy with Cobalt 60 teletherapy units can be calculated by replacing the patient's body cross section in the treatment plane by a suitable idealized body contour, and then integrating the tumour-air ratio around this contour. The resulting integrals have been evaluated for three field sizes as a function of the contour parameters (axial ratio and semi-minor axis). Although the integrals can be evaluated only for tumours located at the center of the contour, an 'eccentricity' correction factor has been developed, thereby extending the method to off center tumours. In the majority of rotation cases, however, this small correction can be neglected.

ZUSAMMENFASSUNG

Der mittlere Intensitätsfaktor (Tiefendosis/Einfallsdosis) für Rotationsbestrahlung mit einem Strahlenwinkel von 360° kann berechnet werden indem man den Körperquerschnitt des Patienten in der Behandlungsflache mit einem entsprechenden idealisierten

Körperumriss ersetzt, so dass der Intensitätsfaktor über diesen Umriss integriert werden kann. Die so aufgestellten Integrale sind für drei Feldgrössen für Cobalt 60 als eine Funktion der Umrissparameter (Länge zu Breite Verhältnis und Breite) ermittelt worden. Obzwar die Ermittlung der Integrale nur für zentral gelegene Tumoren möglich ist, kann die angegebene Methode auch bei Fällen mit anders gelegenen Tumoren angewandt werden, wobei dann ein empirischer Korrektionsfaktor zur Anwendung kommt. Da der Korrektionsfaktor jedoch nur in extremen Fällen von Bedeutung ist kann er meistens vernachlässigt werden.

RÉSUMÉ

On peut calculer le rapport moyen des doses tumeur-air en radiothérapie rotatoire à 360° avec les appareils de télécobaltthérapie en remplaçant la section transversale du corps du malade dans le plan de traitement par un contour convenablement simplifié, et en intégrant le rapport tumeur-air le long de ce contour. Ces intégrales ont été calculées comme des fonctions des paramètres du contour (rapport des axes et demi petit axe) pour trois dimensions de champs. Bien qu'on ne puisse calculer ces intégrales que pour des tumeurs situées au centre du contour, les auteurs ont établi un facteur de correction d'excentricité, permettant d'étendre cette méthode aux tumeurs situées à distance du centre. Cependant, dans la majorité des cas de thérapie rotatoire, cette petite correction peut être négligée.

REFERENCES

Inch, W. R. and Haynes, R. H.: The use of an idealized body contour and integrated transit dose mesasurement for calculating tumour dose in rotation therapy. VIII Internat. Congr. Radiol., Mexico 1956.

Johns, H. E.: The physics of radiation therapy. Charles C. Thomas, Springfield 1953.

— Morrison, M. T. and Whitmore, G. F.: Dosage calculations for rotation therapy; with special reference to cobalt 60. Am. J. Roent. Rad. Ther. Nuc. Med. 75 (1956), 1105.

— Whitmore, G. F., Watson, T. A. and Umberg, F. H.: A system of dosimetry for rotation therapy with typical rotation distributions. J. Canad. Ass. Radiol. 4 (1953), 1.

Neumann, W. und Wachsmann, F.: Ermittlung der Herddosis bei Rotationsbestrahlung unter Berücksichtigung der Absorptionsunterschiede im Gewebe. Strahlentherapie 71 (1942), 438.

Pfalzner, P. M. and Inch, W. R.: Rotation therapy with a Cobalt 60 unit: physical aspects of circumaxial rotation. Acta radiol. 45 (1956), 51.

FROM THE RADIOBIOLOGICAL LABORATORY, RADIUM CENTRE (MEDICAL DIRECTOR: PROF. JENS NIELSEN), COPENHAGEN, DENMARK

STEROL SYNTHESIS AFTER WHOLE BODY ROENTGEN IRRADIATION

by

H. K. Hanel, G. Hjort, G. Johansen and P. R. Purser

I. Cholesterol synthesis from 2-C^{14}-acetate in mouse liver *in vivo*

The purpose of the investigation was to study the effects of whole body roentgen irradiation on cholesterol synthesis from 2-C^{14}-acetate in mouse liver *in vivo*.

GOULD (7) finds an increase in liver cholesterol synthesis after 2,400 r whole body irradiation, ten times higher than normal after 24 hours and 25 to 30 times higher after 48 hours. He regards the increase as a response of the whole animal rather than of the enzyme molecules of the liver. It seems to us that a much lower dose (of the order of the 50 % lethal dose) might produce different reactions from those observed by GOULD and bear more relation to the 'radiation sickness'.

Experimental

Male grey mice of the strain DLB weighing 19 to 21 g, 6 to 7 weeks of age, were used in this investigation. They reared on our standard diet 'mouse cake', containing 0.41 mg cholesterol per g cake.

Submitted for publication 6 March 1957.

Radiation. The mice were given 400 r (0.95 mm Cu HVL) with a dose rate ca 50 r/min, and were restrained in cardboard cages during the irradiation. Irradiated animals were taken after 1 day, 3 days and 7 days, injected intraperitoneally with 20 μC of 2-C^{14}-sodium acetate, and six hours later killed and exsanguinated. Unirradiated mice were taken as controls. The livers were taken out, gall bladders removed, and the livers lightly dried with blotting paper and weighed.

Cholesterol synthesis. The whole livers were saponified, the cholesterol extracted and precipitated as described by HANEL et coll. (3). The resulting cholesteryl digitonide was oxidised by the method of BARKER (1) using VAN SLYKE's mixture (9) and the barium carbonate was suspended in ethyl alcohol and plated on aluminium planchettes. Parallel cholesterol determinations were carried out after the method of HANEL and DAM (4), using acetyl chloride and zinc chloride as reagents for cholesterol.

The barium carbonate samples were counted with an end window G. M. counter and the following corrections made: dead time, background, efficiency and self-absorption, in the last case the specific activity was calculated for a standard 15 mg per cm^2 sample from an experimental self-absorption curve. The results were expressed as cholesterol weight in mg per g liver, specific activity of barium carbonate produced from oxidised cholesteryl digitonide as cpm/mg, and total activity in synthesised cholesterol per g liver, which is taken as a measure of synthesis rate.

Histological technique. Small specimens from the mice livers were taken and fixed in spir. formalini and processed after the ordinary routine histological method; the sections were stained in hematoxylin and eosin.

Autoradiographic technique. Other liver specimens from the mice injected with C^{14}-acetate were fixed in a 10 % aqueous formalin solution containing 1 % $CdCl_2$ and 1 % $CaCl_2$ and embedded in carbowax. Three to four sections (thickness 5 μ) were placed on a slide. Another series of slices from the same liver specimens were fixed in formol alcohol, extracted for lipids and embedded in paraffin. The slices were then coated with Kodak autoradiographic stripping emulsion and exposed for 12 days (6) after which time they were developed and fixed. After mounting, the sections were investigated by phase contrast.

The developed grains and the liver cells were counted per arbitrary square unit from each slide with the aid of an ocular counting grid. The number of grains per cell was then calculated.

Results and discussion

Cholesterol synthesis. The incorporation of 2-C^{14}-acetate in cholesterol shows a significant decrease during the first day after irradiation, with a subsequent increase, though not significantly above normal (Diagram 1).

The cholesterol concentration, or pool size, in liver shows an immediate fall at 6 hours, a rise above normal at 1 day, and a continuous fall again. These changes are obviously not due to change in synthesis rate and must therefore be caused by a changing metabolic rate of cholesterol. The variation in synthesis rate after 6 hours can be explained as a direct effect of the pool size, but the initial drop would seem to be a direct effect of the irradiation. We cannot yet say if this effect is intrinsic or not and experiments are planned to study the effect of the thyroid gland on these phenomena.

The relation of synthesis rate and pool size is shown in Table 1.

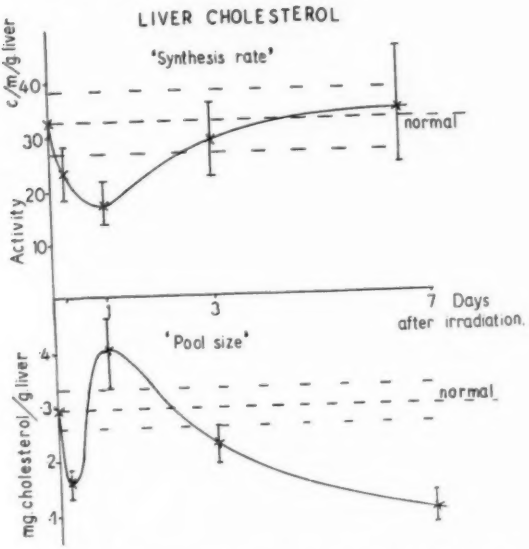

Diagram 1. Cholesterol synthesis rate and cholesterol pool size in liver as function of time after whole body irradiation.

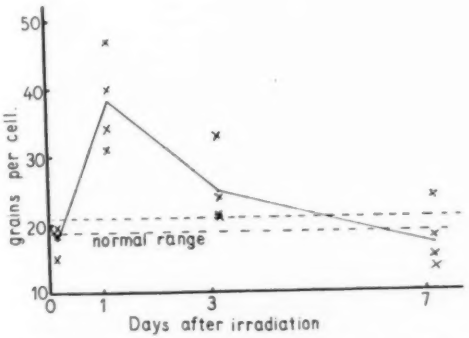

Diagram 2. Grain count per cell in relation to time after irradiation.

Table 1.

Cholesterol synthesis in mouse liver before and after whole-body irradiation

Time after irradiation	Number of animals in group	Cholesterol specific activity c/m/mg Average	Cholesterol concentration in liver mg/g Average	Activity synthesised per g liver c/m Average
6 hours	8	3.65±0.65	0.154±0.025	23.2± 5.3
1 day	6	1.02±0.19	0.404±0.065	17.2± 4.2
3 days	8	3.11±0.53	0.225±0.036	29.3± 6.7
7 days	6	8.50±0.67	0.098±0.030	34.8±10.8
Control, unirradiated	12	2.64±0.34	0.293±0.035	32.4± 5.8

Histology. In livers from mice 1 and 3 days after whole body irradiation there were no significant morphological changes as compared with normal animals. In mice livers 7 days after 400 r a few cells showed nuclear changes such as chromatin clumping, bridge formation and pyknotic nuclei some of which show vacuolisation, as illustrated in Figs. 1—5. By estimation, less than 1 % of the liver cells showed these changes. GEREBTZOFF and BACQ (2) found protoplasmic degeneration 6 hours and 4 days after 700 r whole body irradiation. We were unable to find these changes in our experiments. RHOADES (8) did not find any changes in mice livers 5 to 65 days after 350 r whole body irradiation.

From the histological findings we can conclude that there were no significant variations in cell population and only slight changes in morphology induced by 400 r whole body irradiation.

Autoradiography. The number of grains per cell in the carbowax sections should represent the total activity incorporated. The difference in numbers of grains between the two types of sections should represent the free lipid activity. We found however that the difference was not significant; this may be due to the relatively low incorporation of activity in the free lipids and insufficient extraction of the free lipid precursors which are protein-bound. The grain count per cell represents the incorporation of acetate in total cell components; the relation with time after irradiation is shown in Diagram 2.

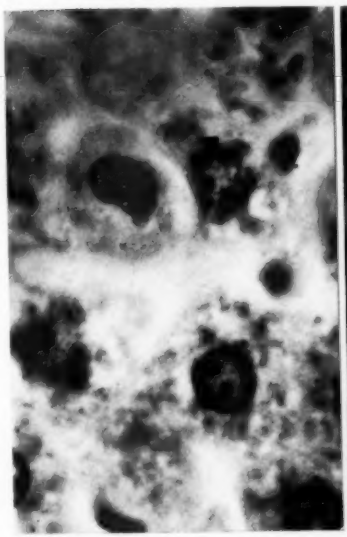

Fig. 1.

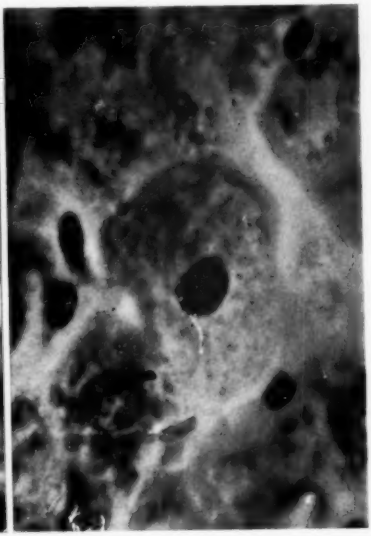

Fig. 2.

Fig. 3.

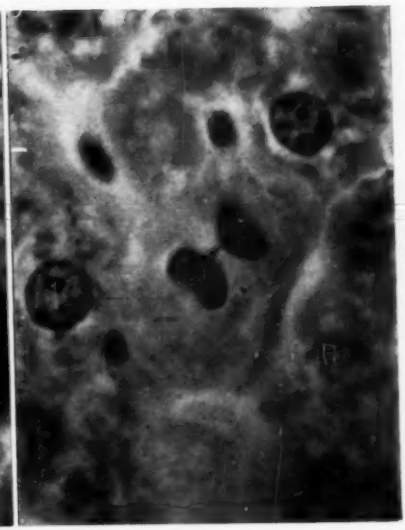

Fig. 4.

Figs. 1—4. Microphotographs from liver cells after 400 r whole body irradiation. Enlargement 1,200 ×.

Fig. 5. Microphotograph from liver cells after 400 r whole body irradiation. Enlargement 1,200 ×.

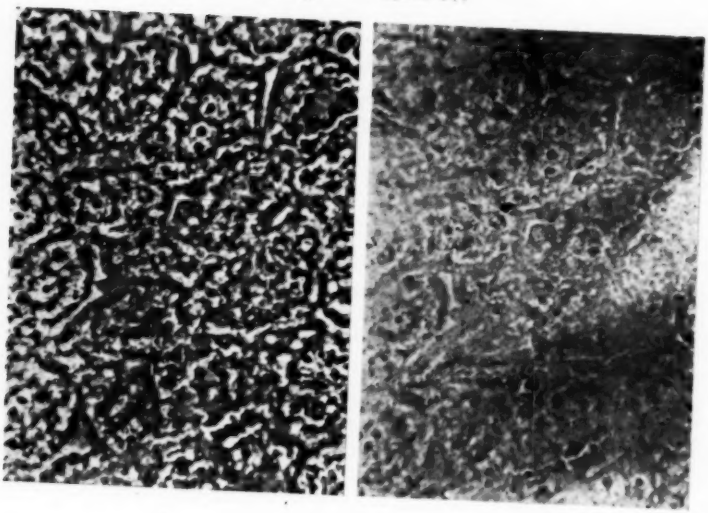

a b

Fig. 6. a) Phase contrast microphotograph from unstained liver section. b) Corresponding photograph in another plane shows the dark silver grains in the autoradiographic emulsion. These pictures are typical of the whole series of experiments. Enlargement 800 ×.

II. Cholesterol synthesis from 2-C^{14}-acetate in rat liver in vitro

Our previous findings showed that whole body roentgen irradiation introduced changes in liver cholesterol metabolism. The purpose of this investigation was to show this effect *in vitro*. Furthermore the study *in vitro* was extended to the measurement of total expired carbon dioxide and its activity, which necessarily corresponds to the metabolised amount of the radioactive substrate.

Experimental

Male, white Wistar rats, weighing about 160 g, 7 to 8 weeks of age, were used in this investigation. They were reared on our standard 'mouse cake' containing 0.41 mg cholesterol per g cake.

Radiation. The rats were restrained in wooden boxes and given a roentgen dose of 400 r (0.95 mm Cu HVL, 50 r/min). Irradiated animals were killed immediately, 1 day, 3 days and 7 days after irradiation. Untreated animals were taken as controls. The animals were killed by fracture of the neck and exsanguinated. The livers were taken out immediately and kept in ice-cold, oxygen-saturated Krebs phosphate buffer pH 7.3 (5).

Cholesterol synthesis. Three analyses were carried out on each liver, two parallel incubations with radioactive acetate and one photometric determination of cholesterol. Slices of about 0.5 mm thickness were prepared by hand, gently dried on filter paper and weighed. Two samples of approximately 2 g of liver slices were put into specially designed incubation flasks (Fig. 7) with an incubation medium consisting of 15 ml phosphate buffer (as above) and 200 μl of a sodium acetate solution containing 20 μC 2-C^{14}-acetate and 10 μ moles inactive sodium acetate. A further sample of about 1.5 g of liver slices was set aside for cholesterol determination.

Carbon dioxide expired during the incubation time was absorbed by 1 ml 10 % NaOH in the central cup; and the process was interrupted after four hours by transferring 1 ml 1-n sulphuric acid from the side arm into the incubation medium, this also liberated dissolved carbon dioxide. The flasks were left overnight to complete the absorption of carbon dioxide, then the NaOH solution was quantitatively transferred to a beaker, 8 mg Na_2CO_3 added as carrier, the carbonate precipitated with excess $BaCl_2$, filtered, dried, and weighed. A sample was then plated out for activity measurement.

For saponification of the liver slices we added ethyl alcohol and potassium hydroxide to the incubation medium so that the final solution contained 50 % alcohol and 17 % hydroxide. The mixture was heated for 8 to 10 hours on a steam bath and the alcohol then evaporated. The unsaponifiable fraction was extracted with petroleum ether (bp. under 50° C) and the sterols precipitated with digitonin as described by HANEL et coll. (3). The precipitated digitonide was washed by centrifuging, twice with 2 ml ether-acetone (1:2), and once with 2 ml ether, and finally dried at 60° C. The total dry precipitate was dissolved in hot ethyl alcohol, quantitatively transferred to a combustion flask, the alcohol completely evaporated in vacuo at 60° C and oxidised as described by BARKER (1) using VAN SLYKE's mixture (9). After absorption of the carbon dioxide in 0.25-n $Ba(OH)_2$ the excess hydroxide was titrated with 0.1-n HCl using phenolphthalein as indicator. From the titration we calculated the amount of sterol. A sample was then plated out for activity measurement.

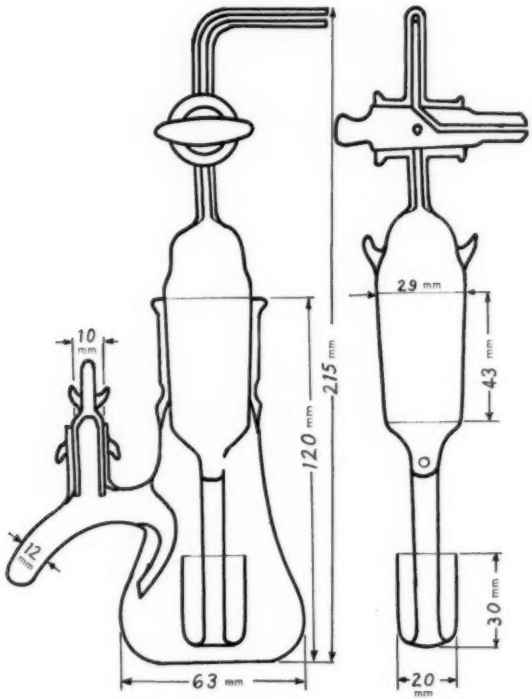

Fig. 7. Incubation flask for liver slices. (Made to our design by Buch & Holm A. S., Copenhagen.)

Table 2.

In vitro synthesis and respiration rate in rat liver after 400 r whole body roentgen irradiation

Days after 400 r	Number of animals in group	Cholesterol mg per g liver before incubation Average	Sterol mg per g liver after incubation Average	Total sterol activity per g liver × 10^{-3} cpm/g Average	Expired CO_2 as mg $BaCO_3$ per g liver Average	Total expired CO_2 activity per g liver × 10^{-3} cpm/g Average
control	5	0.321±0.049	0.469±0.037	6.97±0.33	24.3±1.1	1.12±0.11
0	4	0.363±0.030	0.518±0.007	10.1 ±1.1	23.1±1.4	1.33±0.12
1	2	0.343	0.51 ±0.13	5.3 ±0.5	25.6±0.9	1.62±0.05
3	2	0.285	0.464±0.012	2.12±0.26	30.0±0.3	2.07±0.07
7	2	0.254	0.474±0.023	7.43±0.95	30.6±2.1	1.63±0.14

Calculations. The activity measurements were made with a thin window G. M. tube and corrections were made for counter dead time, background, efficiency, and self-absorption, in the last case the specific activity was calculated for a standard 10 mg per cm² sample from an experimental self-absorption curve.

The cholesterol determination was carried out by the method of HANEL and DAM (4) which is based on the Tschugaeff colour reaction.

The total activities per g liver are calculated by multiplication of the specific activity of barium carbonate by the total amount of barium carbonate in the sample. In the case of sterol activity as shown in Table 2 we took the amounts of barium carbonate corresponding to the steryl digitonide.

For each group of animals the mean is given and the accuracy of the mean calculated as follows

$$\text{variance, } s^2 = \frac{1}{n-1}\sqrt{\sum x^2 - \frac{1}{n}(\sum x)^2}$$

$$\text{accuracy} = \sqrt{\frac{s^2}{n}}$$

where x is one result, and n the number of results.

The results are shown in Table 2 and Diagrams 3 and 4.

Results and discussion

It has been shown that the colour reaction (4) used to obtain the results in the third column of Table 2 is specific to cholesterol, when applied to the unsaponifiable fraction. The digitonide precipitation will determine all sterols with a free hydroxyl group in the 3β-position (*e. g.* $\triangle^{5,7}$-cholestadienol-3β, cholestanol-3β). The colour reaction was made on slices which were not incubated; the digitonide determination was made after incubation. The difference between the two determinations is not entirely due to the synthesis of cholesterol during incubation, as was demonstrated by a preliminary investigation in which colour reaction and digitonide determinations were carried out on incubated and non-incubated slices. These results are shown in Table 3.

It might be expected that the cholesterol concentration 'pool size', would influence the synthesis rate, a change in pool size causing an opposite change in synthesis rate. This would appear to be shown later than three days after irradiation; but there also appears to be a rise in synthesis rate immediately after irradiation, which is not controlled by the pool size, since this increases too. The initial increase in synthesis rate is therefore probably an effect of the irradiation.

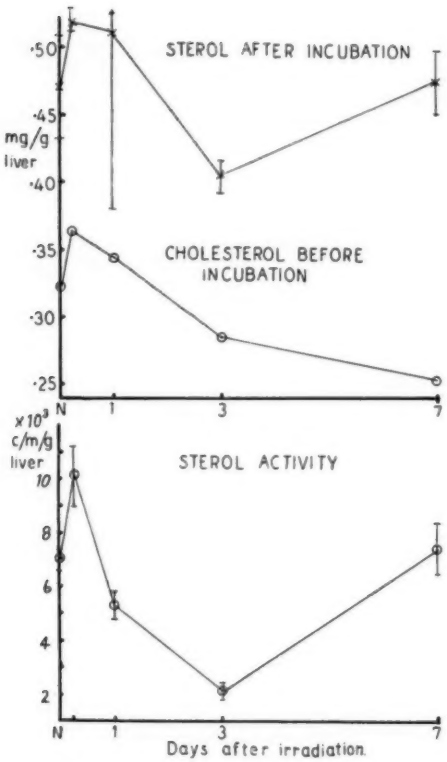

Diagram 3. Incubation of rat liver slices after 400 r whole body irradiation. Sterol concentration and activity.

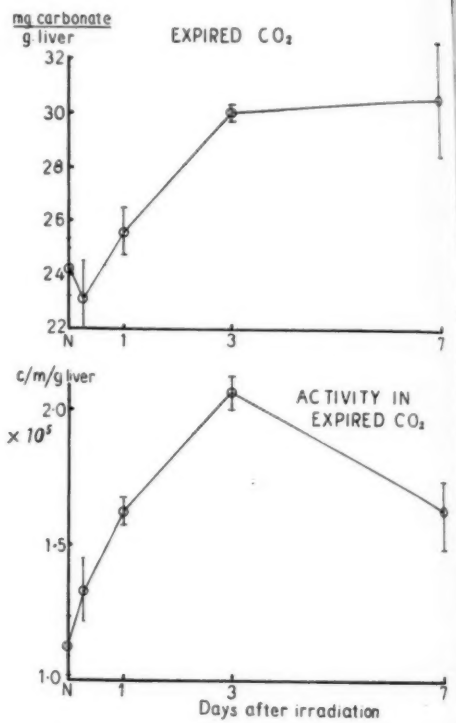

Diagram 4. Incubation of rat liver slices after 400 r whole body irradiation. Expired CO_2 amount and activity.

The graph of sterol concentration after incubation follows that of the sterol synthesis rate, as might be expected. Further experiments are necessary to make deductions from the difference between cholesterol concentration before incubation and sterol concentration after incubation, similar to the experiments which gave the results in Table 3.

The output of carbon dioxide appears to rise slightly after irradiation reaching a maximum at about three days. This is paralleled by a large increase in the activity found in the carbon dioxide.

Histological examination showed a small number of pyknotic nuclei 3 and 7 days after irradiation; a few chromosomal bridges were also found. The proportion of cells showing morphologic changes is so small, that the bicchemical findings cannot be ascribed to this cause.

Table 3.

Concentrations of cholesterol and total sterol in liver slices before and after incubation. All amounts are as mg/g wet liver

	Cholesterol by colour reaction	Sterol by digitonin precipitation	Sterol other than cholesterol
After incubation	0.589	1.136	0.547
Without »	0.191	0.789	0.598
Synthesised sterol	0.398	0.347	

Acknowledgements

The authors wish to thank Miss K. Høegh and Mr. M. Poulsen for valuable technical assistance.

SUMMARY

Male rats were irradiated with 400 r whole body irradiation. The *in vivo* incorporation of 2-C^{14}-acetate in liver cholesterol decreases during the first day after irradiation and subsequently increases. The hepatic cholesterol concentration falls immediately, rises above normal and slowly falls again. Histology shows no change in cell population. Total radioactivity incorporated in liver tissue, as shown by autoradiographs reaches a maximum at 1 day after irradiation.

Incubation of rat liver slices with 2-C^{14}-acetate shows an increase in the metabolism of acetate to carbon dioxide, and an initial increase followed by a fall in the synthesis of digitonine-precipitable sterols from acetate.

ZUSAMMENFASSUNG

Männliche Ratten erhielten Ganzkörperbestrahlung mit 400 r. Die Einverleibung *in vivo* von 2-C^{14}-Acetat in das Lebercholesterol nimmt während der ersten Tage nach der Bestrahlung ab und steigt danach allmählich an. Die Konzentration des Hepaticuscholesteroles fällt sofort ab, steigt dann über das Normalniveau und wird langsam wieder geringer. Die histologische Untersuchung zeigt keine Veränderungen der Zellpopulation. Die totale in das Lebergewebe eingeführte Radioaktivität erreicht, wie Autoradiographien zeigen, ein Maximum einen Tag nach der Bestrahlung.

Bezüglich der Inkubation der Rattenleber zeigen Präparate mit 2-C^{14}-Acetat eine Steigerung des Metabolismus von Acetat zu Kohlendioxyd und eine initiale Zunahme mit nachfolgender Abnahme der Synthese von digitoninfällbaren Sterolen aus dem Acetat.

RÉSUMÉ

Des rats mâles ont subi une irradiation de tout le corps par 400 r. L'incorporation *in vivo* de 2-C^{14}-acétate dans le cholestérol du foie diminue pendant le jour qui suit l'irradiation, puis augmente par la suite. La concentration du cholestérol hépatique

tombe immédiatement, s'élève au dessus de la normale puis redescend ensuite lentement. L'histologie ne montre pas de modification de la population cellulaire. La radioactivité totale incorporée dans le tissu hépatique, mise en évidence par les autoradiographies, atteint son maximum un jour après l'irradiation.

La mise à l'étuve de tranches de foie de rat marquées par le 2-C^{14}-acétate montre une augmentation de la transformation métabolique de l'acétate en gaz carbonique, et une augmentation initiale suivie d'une baisse de la synthèse des stérols précipitables par la digitonine à partir de l'acétate.

REFERENCES

1. Calvin, M., Heidelberger, C., Reid, T. C., and Tolbert, B. M.: Isotopic carbon, p. 92. John Wilhey, New York 1954.
2. Gerebtzoff, M. A., and Bacq, Z. M.: Examen histopathologique de souris irradiées après injection de cystéamine. Experientia 10 (1954), 341.
3. Hanel, H. K., Christensen, F., and Dam, H.: Alimentary production of gallstones in hamsters. IV. Acta path. microbiol. scand. 35 (1954), 237.
4. — and Dam, H.: Alimentary production of gallstones in hamsters. V. Acta chem. scand. 9 (1955), 677.
5. Krebs, H. A., und Henseleit, K.: Untersuchungen über die Harnstoffbildung im Tierkörper. Ztschr. phys. Chem. 210 (1932), 33.
6. Lejtha, L. G.: High resolution autoradiography. Isotope uptake of individual cells. J. Photograph. Science 2 (1954), 130.
7. Progress in Radiobiology. Proc. IVth Intern. Confer. Radiobiology, p. 71. Oliver and Boyd, Edinburgh 1956.
8. Rhoades, R. P.: Histopathology of irradiation from external and internal sources, p. 128. Ed. by W. Bloom. McGraw-Hill, New York 1948.
9. van Slyke, D. D., Plazin, J., and Weizinger, I. R.: Reagents for the van Slyke-Folch wet carbon combustion. J. biol. Chem. 191 (1951), 299.

BOOK REVIEWS

ACTIONS CHIMIQUES ET BIOLOGIQUES DES RADIATIONS. Collection dirigée par M. Haissinsky. Deuxième série. 222 pages, 39 figures. Masson et Cie., Paris 1956. 3,400 fr.

The second volume in this valuable series has now appeared, the three chapters on chemical effects produced by ionizing radiation in the gas phase, luminescence phenomena, and dosimetry, being written by MUND, AGERE, and MILLER, respectively. The first two chapters cover fields which are only rarely dealt with in textbooks, for example the kinetics of a number of inorganic and organic reactions in the gas phase and the theoretical and practical implications of phenomena of importance in the appreciation of the principles of scintillation measurements. The chapter on dosimetry is written with a view to giving a theoretical background for the measurement of ionizing radiation rather than considering technical and instrumental devices employed *e. g.* in roentgentherapy. The reader is presented a good survey in a compressed form and with plenty of numerical data.

This volume should be of considerable value for workers in the fields of radiation physics, chemistry, and biology.

A. Forssberg.

PROGRESS IN RADIOBIOLOGY. Proceedings of the Fourth International Conference on Radiobiology held in Cambridge 14th—17th August 1955. Ed. by J. S. Mitchell, B. E. Holmes, and C. L. Smith. 557 pages, 191 illustrations. Oliver and Boyd, Edinburgh 1956. 63 sh.

This volume of some 550 pages covers over 70 papers and includes discussions on a great number of subjects. It is not possible to give a detailed survey of the many interesting papers but certain items of particular importance in medical radiology may just be mentioned. English and American experiences are presented of the incidence of leukaemia in irradiated patients, particularly in those with ankylosing spondylitis, and, respectively, the response of persons accidentally exposed to fall-out radiation following thermonuclear explosions. The radium content of the body and blood changes in human subjects following contamination with radioactive material, as well as the effects of roentgen irradiation on the human bone marrow, are also discussed. Another group of papers deal with haemopoietic data in animal experiments.

A particular section is devoted to the radiobiology of bone, including reports on lesions from Sr^{90} deposits, development of tumours, and similar matters. There are five experimental reports on the subject of radiation carcinogenesis.

Considerable interest is devoted to the so-called oxygen effect, *i. e.* the fact that radiation damage increases with increasing oxygen tension in cells and tissues as well as to the subject of chemical protection. Reports on the clinical application of the oxygen effect in radiotherapy have actually appeared elsewhere in the literature. A great number of papers in the fields of radiation physics, chemistry, and genetics are also included.

The discussions, which form an important part of the book, add considerably to the value and usefulness of this well edited and beautiful volume.

A. Forssberg.

RÖNTGENDIAGNOSTIK. Ergebnisse 1952—56. Herausgegeben von H. R. SCHINZ, R. GLAUNER und E. UEHLINGER, 590 S., 550 Abb. Georg Thieme Verlag, Stuttgart 1957. DM. 139.—.

This work, which was firmly established before the war with papers both on diagnosis and therapy, now appears with these two fields separated. This is a sensible move. The publication comprises a number of valuable articles of special interest to those who have studied Volume V of the textbook by SCHINZ-BAENSCH-FRIDL-UEHLINGER and with which 'Ergebnisse' is closely connected.

The first chapter, 'New aspects of the spine' by BROCHER, is comprehensive and detailed. Congenital cervical anomalies are particularly well described although fractures and traumatic lesions which are so important in this portion of the spine are not mentioned.

Various forms of bone cyst are well presented by UEHLINGER. Heart function is discussed by ZDANSKY, but the text makes heavy reading and the subject matter is difficult to follow. JANKER is the author of an interesting chapter on angiocardiography in congenital heart disease; only a few cases, however, were examined selectively with injection of the contrast medium through a catheter. Abdominal aortography, presented by WELLAUER, consists mostly of cases examined by the translumbar technique. It may be stated that catheter replacement constitutes a better technique and it is noted that the new selective type of examination with a curved tip of catheter is not mentioned.

Arteriography of the extremities is performed by means of injection through a needle. Despite the excellent illustrations and attention to detail, the method in the reviewer's opinion is out of date. The chapter on lieno-portal venography is not of the highest standard and the reviewer must again object to the technique of using a needle in place of a tube for the injection. Better results are also obtained with an automatic film changer. Vertebral angiography is well presented by YSARGIL and many valuable details are given. Among the many competent chapters on the gastro-intestinal tract, mention must be made of those by PREVOT and WELIN whose contributions are outstanding. Retroperitoneal pneumography and pneumomediastinum are well covered by COCCHI and should be carefully studied by those who intend to undertake such procedures. The final chapter on hystero-salpingo-pelviography written by NORMAN is particularly praiseworthy and of great interest.

To summarize, it may be said that the book can be strongly recommended to diagnostic radiologists. Many will find it difficult to do without it. The printing and illustrations are excellent and the references give the book additional value. In future editions one may hope for a more critical selection of papers, for fresh ideas, and for new approaches.

J. Frimann-Dahl.

FRAKTUREN IM KINDESALTER. Von Hans Rettig. 92 S., 196 Abb. in 330 Einzeldarst. Verlag von J. F. Bergmann, München 1957. DM. 26: 80.

This book is a short systematic account of diagnosis, therapy and complications in the most common fractures in newborns, infants and children up to puberty. It is pointed out that skeletal injuries in these age groups offer many diagnostic and therapeutic problems that are not satisfactorily dealt with in most current text-books of fractures. Although the main part of this book is devoted to treatment, it has interest for radiologists because of the rich material of reproductions of roentgenograms. These are generally of good quality and illustrate well the changes mentioned in the text. The value of roentgen examination of the healthy extremity for comparison of suspected epiphyseal injuries is emphasized, but a more detailed description of normal variations of skeletal development that may cause diagnostic difficulties is obviously not within the scope of this book. Multiple references enhance its usefulness. It is strongly recommended.

Ulf Rudhe